ASTRONOMY & ASTROPHYSICS
SUPPLEMENT SERIES

JULY **1986,** PAGE 145

Astron. Astrophys. Suppl. Ser. **65,** 145-188 (1986)

VLA observations of low luminosity radio galaxies. III. The A-array observations

C. Fanti ([1,2]), R. Fanti ([1,2]), H. R. de Ruiter ([1]) and P. Parma ([1])

([1]) Istituto di Radioastronomia, Via Irnerio, 46, 40126 Bologna, Italy
([2]) Dipartimento di Astronomia, Universita' di Bologna, Via Zamboni, 33, 40126 Bologna, Italy

Received September 16, accepted November 5, 1985

Summary. — We present radio observations of 65 radio galaxies, made with the VLA A-configuration, at 20 cm. The angular resolution is about 1.5 arcsec. The sources were selected from two samples of low luminosity B2 radio galaxies recently observed with the B and/or C configuration of the VLA (Parma *et al.*, 1986 ; de Ruiter *et al.*, 1986). The criterion of selection for observation with the A array was either that the source had small angular size, not adequately resolved by the VLA observations at lower resolution, or that the source contained a significant fraction of the flux in unresolved or barely resolved components. The data presented here provide significant information on radio cores, jets and other compact features (e.g. : radio knots, hot spots). As in previous papers, we give in separate tables the observational parameters for each source. Intrinsic source properties, such as equipartition parameters etc..., will be given in a subsequent paper. We also present contour maps for the majority of the sources. Information on individual sources is provided, particularly in case of interesting structures.

Key words : radio galaxies.

1. Introduction.

This is the third of a series of papers aimed at studying with the VLA, at 20 cm, the radio structure of radio galaxies in two complete B2 samples (defined in Colla *et al.*, 1975 — the « bright » sample — and Fanti *et al.*, 1978 — the « faint » sample).

Previous papers (Parma *et al.*, 1986 ; de Ruiter *et al.*, 1986, in press, hereafter referred to as Paper I and Paper II), reported VLA observations of sources respectively mostly smaller (B array) or larger (C array) than two arcmin. On the basis of those data, we selected 65 radio galaxies for additional observation with the A configuration of the VLA, to allow the study at higher resolution of radio features (such as cores, knots, jets, hot spots) which were not mapped with the proper resolution in the previous observations.

In the near future we will give further B array maps of a few sources and will present there, in a systematic way, the whole set of data (Paper IV).

In section 2 we describe the observations and the data reduction procedure.

In section 3 we give the results in the form of radio contour plots and of tables, in which the observed parameters are summarized.

Finally, in section 4, comments are given on a number of sources.

Send offprint requests to : C. Fanti.

2. Observations and data reduction.

A description of the VLA and its modes of operation can be found in Thompson *et al.* (1980).

The observations were done in december 1984. Each source was observed for 10 to 30 min, at the frequencies of 1435 and 1665 MHz, both with a bandwith of 25 MHz.

The resulting full width at half maximum of the synthesized beam is about 1.5 arcsec at 1435 MHz and proportionally smaller at 1665 MHz.

A calibration source was observed immediately before or after a program source. The flux densities were brought on the scale of Baars *et al.* (1977), using 3C 48 and 3C 286 as primary flux calibrators. Flux densities of other calibration sources were bootstrapped from the flux densities of 3C 48 and 3C 286. Raw data were checked for deviating amplitudes, which were edited out.

Post-calibration reduction was done using the NRAO AIPS package running on the Vax 11/780 of the Institute of Radio Astronomy, equipped with an Array Processor FPS 5310 of the Department of Astronomy. The procedure followed was identical to the one described in paper I.

Confusion problems were generally absent. Only in a minority of cases confusing sources were present, far from the field center. They were cleaned simultaneously with the source under study using the task MX in AIPS. The clean components thus obtained were subtracted in the UV plane and the process was then repeated on the resulting UV data until convergence was reached.

A number of sources required self-calibration, which generally improved the dynamic range.

Since we are interested mainly in the structure and strength of the radio sources at 20 cm (as in Papers I and II), we present only the 1435 MHz data; we just remark that 1665 MHz data (source parameters and radio maps) do exist.

For a number of sources of large total size we have obtained also maps combining the present observations with those made with the B array (Paper I) or the C array (Paper II). The UV data were merged and a uniform weight was applied to them. Such combinations produce maps free from large scale negative sidelobes which hide interesting features and therefore contain a lot more of information than the A and C (or A and B) maps alone. The effective beamshape and r.m.s. noise are similar to those given in tables Ia and Ib for the A-array maps.

The r.m.s. noise in the final map is for most fields in the range 0.1 to 0.2 mJy/beam, which is generally comparable to the receiver noise.

Following paper I we list in tables Ia and Ib the observational parameters for the bright and faint sample respectively. We give the source name, the observing time per source, the FWHM of the synthesized beam and the r.m.s. noise in the final 1435 MHz map. Polarization maps were obtained for a number of sources and will be analysed in a separate paper.

Three sources (0222+36, 0258+35, 0331+39) have been observed also at 5 GHz with a resolution of about 0.4 arcsec. The corresponding observational parameters are also given in table I.

3. Results.

Source parameters, computed as explained in paper I, are given in tables IIa and IIb for the 20 cm and in table III for the 6 cm data. The organization of these tables is identical to the one of table II in paper I.

The total intensity and overall angular size are taken from the previous papers (I or II in parentheses next to the flux), whenever the present observations have resolved the radio structure too much.

We give data only for relatively compact features, for which we expect that the A array observations had no significant flux losses. For parameters relative to large emission regions we refer to papers I and II.

One source (1358+30), mapped with the C array (Paper II), was not detected at all and is not listed in table II.

In figure 1-72 we present contour maps. When A array and C array (or B array) data were combined, as described in section 2, we present the combined maps.

There are a few cases where the proposed optical identification seems rather far from the radio source (e.g. : 0207+38, 1254+27 and 1736+32). We presume, however, that these identifications are correct, and that the larger than usual position differences are due to the large extent of the optical galaxies.

4. Comments on individual sources.

For general comments on the sources we refer to papers I and II. Here only notes based on the present radio data are given.

4.1 THE BRIGHT SAMPLE.

0034+25 The source is of the WAT type, ~ 2 arcmin in size (see Paper II). The present observations allow mapping of the inner part of the source (the inner jet) only.

0206+35 The large halo, visible in the combined map, is completely embedded in the optical galaxy. The galaxy shows evidence of a dust lane (see Paper I).

0800+24 The source is a WAT, about 1.5 arcmin in size. In the present map it is almost completely resolved out, showing only few features in the head.

0836+29A The optical position is taken from Goodson *et al.* (1979).

1040+31 The optical counterpart is a triple system in a common halo. Unfortunately we do not have good positions of the individual galaxies and therefore the interpretation of the structure is difficult. The optical position in figure 1 is from Goodson *et al.* (1979). There seems to be a two-sided jet emanating from a compact component, which terminates in two hot spots.

1108+27 Our B array map (Paper I) showed a faint jet east of the core, not visible here.

1626+39 See Burns *et al.* (1983) for a discussion of the source.

4.2 THE FAINT SAMPLE.

0836+29 The radio source (in Abell 690) has a large angular extent (~ 5.5′). Here we see only the core and the northern radio jet.

0838+32 See paper II for the large scale radio emission of this source.

1005+28 See paper II for the large scale radio emission. The faint weak structure we see corresponds to features within the central component in the map shown in that paper.

1243+26 This source (in Abell 1609) seems to consist of two independent WAT's associated with two separate galaxies of the cluster. Two unresolved sources coincide with the positions of the two galaxies and are likely to be their cores.

1300+32 The galaxy suggested as identification coincides in position with a 0.6 mJy source, probably the core. A faint bridge, not seen here, connects the west component to the northern one, giving the overall appearance of a WAT (see Paper II). Another bright galaxy (originally believed to be the optical identification) coincides with a just barely believable 0.3 mJy source.

1339+26 See papers I and II for the overall structure.

1528+29 See paper II for the double lobed large scale structure, here completely resolved out. The eastern compact component in the present map is the radio core and the western one is a hot-spot. The southern source is likely to be a background object.

1527+30 See paper I for the missing extended structure.

1658+30 See paper II for the missing extended structure. The western weak emission is a resolved hot-spot.

1736+32 The source has a remarkable radio structure that we interpret as superimposition of two unrelated double sources, the NE component of the small (background) one being projected onto the SE lobe of the radio galaxy. In table II the fluxes of the two overlapping components have been roughly separated.

Acknowledgements.

H. de R. and P. P. were visitors at the VLA, during the observation and calibration stage of the program and wish to acknowledge the hospitality of the VLA staff.

The Array Processor FPS 5310, used for the data reduction was financed by the Ministero della Pubblica Istruzione.

The National Radio Astronomy Observatory is operated by Associated Universities, Inc., under contract with the National Science Foundation.

References

BAARS, J. W. M., GENZEL, R., PAULINY-TOTH, I. I. K., WITZEL, A. : 1977, *Astron. Astrophys. Suppl. Ser.* **61,** 99.
BURNS, J. O., SCHWENDEMAN, E., WHITE, R. : 1983, *Astrophys. J.* **271,** 575.
COLLA, G., FANTI, C., FANTI, R., GIOIA, I., LARI, C., LEQUEUX, J., LUCAS, R., ULRICH, M.-H. : 1975, *Astron. Astrophys. Suppl. Ser.* **20,** 1.
FANTI, R., GIOIA, I., LARI, C., ULRICH, M.-H. : 1978, *Astron. Astrophys. Suppl. Ser.* **34,** 341.
GOODSON, R. E., PALIMAKA, J. J., BRIDLE, A. H. : 1979, *Astron. J.* **84,** 1111.
PARMA, P., DE RUITER, H. R., FANTI, C., FANTI, R. : 1986, *Astron. Astrophys. Suppl. Ser.* in press.
DE RUITER, H. R., PARMA, P., FANTI, C., FANTI, R. : 1986, *Astron. Astrophys. Suppl. Ser.* in press.
THOMPSON, A. R., CLARK, B. G., WADE, C. M., NAPIER, P. J. : 1980, *Astrophys. J. Suppl. Ser.* **44,** 151.

TABLE Ia. — *Observational parameters.*

Name	Obs. time min	beam arcsec	PA degrees	noise mJy/beam
0034+25	17	1.63 x 1.60	65	0.14
0149+35 NGC 703	24	1.74 x 1.57	74	0.16
0206+35 4C35.03	29	1.09 x 1.08	43	0.25
0207+38 NGC 828	11	1.21 x 1.14	35	0.24
0222+36	11 (20cm) 8 (6 cm)	1.26 x 1.21 0.36 x 0.35	34 -36	0.16 0.14
0258+35 NGC1167 4C34.09	11 (20cm) 8 (6 cm)	1.38 x 1.39 0.37 x 0.36	45 -31	0.85 0.32
0331+39 4C39.12	26 (20cm) 8 (6 cm)	1.12 x 1.10 0.38 x 0.36	41 -17	0.11 0.12
0648+27	11	1.63 x 1.21	90	0.17
0722+30	30	1.51 x 1.22	73	0.15
0800+24	16	1.89 x 1.63	-73	0.30
0836+29 4C29.30	14	1.49 x 1.35	57	0.18
1040+31 4C29.41	30	1.44 x 1.25	60	0.15
1102+30	20	1.49 x 1.25	62	0.22
1108+27	30	1.39 x 1.32	52	0.12
1113+29 4C29.41	20	1.38 x 1.34	49	0.20
1144+35	10	1.20 x 1.20	43	0.50
1254+27 NGC4839	7	1.51 x 1.48	38	0.08
1317+33 NGC5098	25	1.50 x 1.20	68	0.12
1318+34	19	4.24 x 4.22	-46	0.35
1322+36 NGC5141 4C36.24	18	1.24 x 1.12	62	0.20
1422+26	29	1.40 x 1.20	54	0.10
1506+34	10	1.41 x 1.38	47	0.25
1525+29	28	1.12 x 1.10	41	0.12
1553+24	29	1.20 x 1.17	30	0.12
1621+38 NGC6137	14	1.38 x 1.33	-52	0.27
1626+39 NGC6166 3C338	12	1.61 x 1.61	36	1.40
1855+37	10	1.41 x 1.36	-56	0.27
2116+26	25	1.28 x 1.20	-3	0.16
2236+35	25	1.14 x 1.09	35	0.13

TABLE Ib. — *Observational parameters.*

Name	Obs. time min	beam arcsec	PA degrees	noise mJy/beam
0708+32	29	1.53 x 1.27	77	0.15
0836+29	16	1.96 x 1.58	-82	0.25
0838+32	14	1.53 x 1.32	66	0.19
0908+37	14	1.52 x 1.30	69	0.18
0913+38	19	1.46 x 1.25	61	0.11
0922+36	15	1.76 x 1.56	77	0.45
1003+26	10	1.48 x 1.30	83	0.20
1005+28	11	1.80 x 1.58	-85	0.12
1037+30	10	1.56 x 1.34	71	0.35
1113+24	27	1.13 x 1.12	45	0.10
1204+24	29	1.10 x 1.10		0.08
1204+34	29	1.40 x 1.10	41	0.15
1243+26	19	1.52 x 1.48	40	0.05
1300+32	23	1.51 x 1.47	37	0.07
1303+31	20	1.23 x 1.14	25	0.14
1339+26	14	1.46 x 1.27	75	0.17
1347+28	29	1.42 x 1.29	57	0.07
1357+28	14	1.40 x 1.30	52	0.12
1358+30	15	1.38 x 1.35	48	0.12
1430+25	14	1.40 x 1.40		0.10
1450+28	29	1.12 x 1.11	44	0.10
1457+29	13	1.16 x 1.15	42	0.06
1521+28	15	1.55 x 1.53	37	0.12
1527+30	30	1.16 x 1.13	36	0.14
1528+29	24	1.58 x 1.51	26	0.06
1609+31	22	1.25 x 1.18	-10	0.14
1613+27	21	1.29 x 1.20	-5	0.20
1638+32	19	1.27 x 1.24	36	0.16
1643+27	14	1.74 x 1.72	49	0.15
1658+30	19	1.73 x 1.57	54	0.15
1658+32	19	4.22 x 4.16	22	0.20
1726+31	15	1.69 x 1.67	51	0.70
1736+32	19	1.27 x 1.27		0.24
1747+30	29	1.80 x 1.70	58	0.15
1752+32	30	1.41 x 1.30	-69	0.16
1827+32	14	1.42 x 1.33	-77	0.17

TABLE IIa. — *Observational data.*

NAME	R.A. h m sec	DEC. ° ' "	z	m_{pg}	S(1.4) mJy	Size FWHM arcsec	P.A. deg.	LAS arcsec
0034+25	00 34 26.8	25 25 26	0.0321	14.8	122 (II)			183
NGC 507								
core	00 34 26.77	25 25 26.4			5.4	1.1 x 0.5	96	
0149+35	01 49 50.0	35 54 20	0.0160	14.5	78 (I)			58
NGC 703								
core	01 49 50.02	35 54 20.4			12.7	1.2 x 0.7	44	
0206+35	02 06 39.3	35 33 41	0.0375	14.9	2050 (I)			89
4C35.03								
core	02 06 39.35	35 33 41.6			128	1.2 x 0.2	135	
E jet					144			9
W jet					198			26
0207+38	02 07 07.1	38 57 22	0.0181	13.0	111			17 x 10
NGC 828								
0222+36	02 22 23.9	36 56 57	0.0327	15.0	204			7 x 5
core	02 22 23.94	36 56 56.9			187	0.5 x 0.2	48	
0258+35	02 58 35.6	35 00 31	0.0160	14.0	1815			
NGC1167								
4C34.09								
core	02 58 35.38	35 00 32.0			1780	1.0 x 0.5	116	
0331+39	03 31 01.0	39 11 25	0.0202	14.2	904 (I)			68
4C39.12								
core	03 31 00.95	39 11 23.6			222	0.5 x 0.3	154	
0648+27	06 48 54.9	27 31 18	0.0409	14.9				
core	06 48 54.84	27 31 18			152	< 0.9		
0722+30	07 22 27.5	30 03 14	0.0191	15.6	138			29
Core	07 22 27.51	30 03 14.1			27	0.7 x 0.4	144	
W lobe					57			13
E lobe					54			11
0800+24	08 00 16.3	24 49 02	0.0433	15.7	100 (I)			94
Core ?					1.0			
0836+29A	08 36 59.1	29 59 42	0.0650	15.7	575 (I)			64
4C29.30								
core	08 36 59.01	29 59 41.3			27	< 1.0		
jet					49			25
N h. spot	59.3	53			48	4.5 x 1.5	26	
S h.spot	58.4	26			45	0.9 x 0.6	106	
1040+31	10 40 31.2	31 46 51	0.0360	15.5	770 (I)			54
4C29.41								
core ?	10 40 31.13	31 46 50.6			43	1.0 x 0.5	163	
S hot spot	31.53	35.0			14	1.2 x 0.7	0	
jet?					50			13
N hot spot	30.8	58			3	< 2.5		
1102+30	11 02 39.7	30 25 53	0.072	15.7	335 (II)			170
core	11 02 39.62	30 25 53.8			10	< 1.0		
1108+27	11 08 44.3	27 14 06	0.0331	14.6	87 (I)			72
core	11 08 44.06	27 14 07.2			14	< 0.5		
W jet					56			17
1113+29	11 13 53.4	29 31 34	0.0489	15.1	1810 (I)			91
4C29.41								
core	11 13 53.55	29 31 39.9			34	0.9 x 0.2	78	
W jet					88			26
W hot-spot	11 13 51.3	29 31 35			124			
1144+35	11 44 45.5	35 17 49	0.063	15.7				
core	11 44 45.50	35 17 47.5			568	0.4 x 0.1	28	
1254+27	12 54 59.4	27 46 02	0.0249	13.6	63			34
NGC4839								
core ?	12 54 59.10	27 46 04.8			2.3	< 2		
N jet ?					43			16
S jet ?					18			14
1317+33	13 17 55.8	33 24 19	0.0379	15.0	79			17
NGC5098								
Core	13 17 55.79	33 24 19.0			11	< 0.8		
N lobe					35			8 x 7
S lobe					33			8 x 8
1318+34	13 18 16.9	34 23 56	0.0232	14.8	94			
core	13 18 17.0	34 24 04			84	1.5 x 0.4	146	
1322+36	13 22 35.4	36 38 19	0.0175	13.9	808 (I)			53
NGC5141								
4C36.24								
core	13 22 35.33	36 38 18.7			73	0.7 x 0.1		
S jet					88			24
1422+26	14 22 26.5	26 51 02	0.037	15.6	679 (II)			140
Core	14 22 26.47	26 51 02.3			12	< 0.7		
E jet					12			24
W jet					15			27
1506+34	15 06 05.6	34 34 18	0.0452	15.6	127			
core	15 06 05.33	34 34 49.2			115	0.5 x 0.3	33	

TABLE IIa *(continued)*.

NAME	R.A. h m sec	DEC. ° ′ ″	z	m_{pg}	S(1.4) mJy	Size FWHM arcsec	P.A. deg.	LAS arcsec
1525+29	15 25 39.6	29 06 28	0.0653	15.4	220			23
N lobe+jet					96			11 x 8
S lobe+jet					110			10 x 8
1553+24	15 53 56.3	24 35 32	0.0426	15.4	119 (I)			61
core	15 53 56.18	24 35 32.7			53	< 1.0		
N jet					45			20
S jet					26			15
1621+38	16 21 16.9	38 02 17	0.0310	14.1	395 (I)			57
NGC6137								
core	16 21 16.81	15.0			31	1.1 x 0.4	169	
N blob	16.7	18			14	2.6 x 0.7	160	
S blob	16.8	13			21	1.6 x 1.2	20	
tail					194			35 x 15
1626+39	16 26 55.4	39 39 36	0.0303	13.9	3255 (I)			110
NGC6166								
3C338								
core	16 26 55.31	39 39 36.5			146	0.5 x 0.4	68	
W blob	54.8	37			33	3.0 x 1.3	76	
Sjet+blob	~ 54.4 - 57.5	~ 25			450			23
SW blob	~ 53.5	~ 30			363			13
1855+37	18 55 54.3	37 56 27	0.0552	14.9	273			7
N lobe	54.3	31			82	6.0 x 1.3	64	
central	54.3	28			54			
S lobe	54.2	24			137	2.0 x 1.7	44	
2116+26	21 16 20.7	26 14 08	0.0164	14.0	105 (I)			78
core	21 16 20.80	26 14 08.9			42	0.4 x 0.2	54	
N jet					7			22
S jet					28			19
2236+35	22 36 12.3	35 04 11	0.0277	15.0	348 (I)			47
core	22 36 12.27	35 04 09.4			6.7	0.6 x 0.4	44	
E jet					85			16
W jet					(94)			17

TABLE IIb. — *Observational data.*

NAME	R.A. h m sec	DEC. ° ′ ″	z	m_v	S(1.4) mJy	Size FWHM arcsec	P.A. deg.	LAS arcsec
0708+32	07 08 33.6	32 23 37	0.0672	15.8	58			8
N Lobe	33.6	42			16	1.4 x 1.0	170	
Central	33.58	37.9			22	0.6 x <.6	180	
S lobe	20.3	33.6			20	1.4 x 0.9	160	
0836+29	08 36 13.4	29 01 17	0.079	14.7	591 (II)			325
core	08 36 13.56	29 01 15.3			110	< 0.5		
N jet					110			51
0838+32	08 38 06.8	32 35 39	0.068	14.8	591 (II)			128
N comp.	06.0	45			150			7 x 6
S comp.	06.5	38			220			6 x 5
W wing					68			45 x 15
E wing					82			15 x 10
0908+37	09 08 45.4	37 36 33	0.1040	15.5	626 (I)			51
core	09 08 45.29	37 36 33.0			25	0.7 x 0.5	57	
N jet					134			23
0913+38	09 13 39.1	38 30 41	0.0711	15.7	346 (I)			47
W jet					47			17
0922+36	09 22 34.3	36 40 05	0.1125	15.6	639 (II)			202
core	09 22 34.16	36 40 04.6			8	< 0.4		
S blob	34	39 35			139	7 x 4		
1003+26	10 03 49.4	26 09 24	0.1165	16.5	69			6
S comp	49.4	22			36	2.2 x 0.6	172	
N comp.	49.5	25			33	2.7 x 1.1	162	
1005+28	10 05 06.4	28 16 29	0.1476	16.4	77 (II)			230
jet ?					10			
1037+30	10 37 42.7	30 13 38	0.0908	16.4	360			3
core ?	10 37 42.80	30 13 38.4			260	< 1.2		
E comp	42.90	37.5			98	< 0.8		
1113+24	11 13 24.0	24 57 24	0.1021	15.0	38 (I)			40
N comp.					10			3
S comp.					14			3
1204+24	12 04 34.3	24 11 06	0.0769	15.2	128 (I)			33
core	12 04 34.36	24 11 06.6			12	0.7 x 0.1	166	
1204+34	12 05 00.5	34 09 21	0.0788	15.8	413 (I)			62
core	12 05 00.41	34 09 21.6			17	0.3 x 0.2	124	
WWhot-spot	12 04 58.7	34 09 38			46	5.7 x 2.4	45	
W " "	59.3	34			9	2.6 x 0.9	114	
E " "	05 01.9	07			21	0.9 x 0.9		

TABLE IIb *(continued)*.

NAME	R.A. h m sec	DEC. ′ ″	z	m_v	S(1.4) mJy	Size FWHM arcsec	P.A. deg.	LAS arcsec
1243+26	12 43 54.6	26 43 39	0.0891	15.1	219 (II)			166
	52.7	42 32		16.0	177 (II)			90
N core	12 43 54.65	26 43 39.7			7.7	1.9 x 0.5	34	
N N jet					196			166
N S jet					15.5			
S core	12 43 52.77	26 42 32.0			3.8	0.9 x 0.5		
SW comp.					138			
1300+32	13 00 52.9	32 06 25	0.1639	16.9	304 (II)			165
W tail	~ 53	05 55			195			118
NE comp.	57	06 35			95			33 x 18
N comp.	53.8	06 45			14			12 x 8
1303+31	13 03 28.3	31 10 20	0.1816	16.7	68			16
head	28.2	20			14	1.1 x 0.7	51	
body	28.1	17			38	1.6 x 04	23	
tail	27.9	12			16			7 x 3
1339+26								
head tail	13 39 30.7	26 37 20	0.0757	14.2	320 (II)			198
WAT	29.4	35	0.0688	14.2	21 (I)			24
1347+28	13 47 56.3	28 31 34	0.0724	15.2	198 (I)			54
core	13 47 56.37	28 31 35.5			3.3	< 1.0		
1357+28	13 57 45.2	28 44 28	0.0629	14.6	252 (II)			160
Core	45.16	30.1			6.8	1.6 x 0.6	180	
N jet					65			26
S jet					23			19
1430+25	14 30 26.9	25 08 28	0.0813	15.7	537 (I)			71
N comp	14 30 28.2	25 09 24			105			5
head	27.0	08 30			127			8
tail	27.3	08 40			95			12 x 10
1450+28	14 50 23.8	28 10 05	0.1265	16.5	125 (I)			57
core	23.86	06.5			6	0.9 x 0.2	129	
E jet					39			19
W blob	23.7	08			3	1.2 x 1.0	115	
1457+29	14 57 34.4	29 15 23		17.2	309 (II)			75
Central	34.3	26			29			4.4
1521+28	15 21 21.4	28 48 07	0.0825	15.4	527 (II)			220
core	15 21 21.41	28 48 08.2			44	0.7 x 0.1	142	
jet					93			50
1527+30	15 27 43.3	30 52 49	0.1143	15.0	81 (I)			73
central	15 27 43.3	30 52 50			22	1.3 x 0.5		
1528+29	15 28 05.9	29 10 43	0.0843	15.1	214 (II)			225
core	15 28 05.89	29 10 43.1			2.7	< 1.0		
W hot spot	27 57.84	19.4			1.3	1.1 x 0.7		
1609+31	16 09 42.3	31 10 41	0.0944	15.6	141			25
N lobe					87			10 x 10
S lobe					61			10 x 9
1613+27	16 13 28.9	27 34 21	0.0647	14.9	233			31
core	28.75	22.2			11	1.5 x 0.3		
S lobe+jet					106			15 x 9
N lobe					92			11 x 11
1615+32	16 15 46.9	32 29 49	0.1520	16.7	2547 (II)			93
core	16 15 46.96	32 29 50.5			11	1.2 x 1.1		
N hot spot	47.43	30 24.1			51	1.2 x 0.9	102	
1638+32	16 38 34.9	32 11 09	0.1398	15.8	309 (I)			57
core	34.98	09.9			56	0.8 x 0.2	89	
jet					96			25
1643+27	16 43 26.6	27 25 30			101 (II)			145
core	16 43 26.63	27 25 30.3			5	1.5 X 1.0	17	
N jet					13			13
S hot spot	25.9	07			5.5	2.4 X 1.6		
1658+30	16 58 48.9	30 12 32	0.0351	15.1	571 (II)			
core	16 58 48.94	30 12 33.0			59	< 1.0		
bright jet					8			~ 4
1726+31	17 26 27.4	31 48 25	0.167	16.5	2600 (II)			115
core	17 26 27.32	31 48 24.3			7.4	3.2 x 1.2	136	
1736+32	17 36 45.2	32 57 36	0.0741	15.1	129			32
E lobe					50			
Core	17 36 45.06	32 57 58.9			14	< 1.7		
Twin jets					25			
W lobe					40			
Double					55			16
NE comp.	~ 46.0	~ 30			40			
SW comp.	45.0	25			15			
1747+30	17 47 56.3	30 18 55	0.1297	16.7	49 (I)			98
core	56.30	56.3			4.5	< 1.0		
1rst blob	56.2	19 00.9			2.9	1.3 x 1.2	157	
2nd blob	56.1	08.0			4.7	5.8 x 0.9	177	
1752+32	17 52 44.5	32 34 45	0.0449	14.3	136 (I)			95
Inner jets	44.4	32 34 44			27	~ 4		
1827+32	18 27 04.9	32 17 59	0.0659	15.1	255 (II)			355
core	18 27 05.1	32 18 01.9			26	1.0 x 0.3	75	

TABLE III. — *Observational data at 6 cm.*

NAME	R.A. h m sec	DEC. ' "	S(5.0) mJy	Size FWHM arcsec	P.A. deg.	LAS arcsec
0222+36	02 22 23.9	36 56 57	150			~ 1
core .	02 22 23.94	36 56 56.9	140	0.17 x 0.07	37	
0258+35	02 58 35.6	35 00 31	939			~ 4 x 1.7
NGC1167						
4C34.09						
NW comp.	02 58 35.31	35 00 32.7	176			1.6 x 1.4
SE comp	.37	32.0	757			2.2 x 1.8
0331+39	03 31 01.0	39 11 25	> 350			> 10
4C39.12						
core	03 31 00.95	39 11 23.7	149	< 0.3		
S ext.	.95	23.51	66	0.6 x 0.2	165	

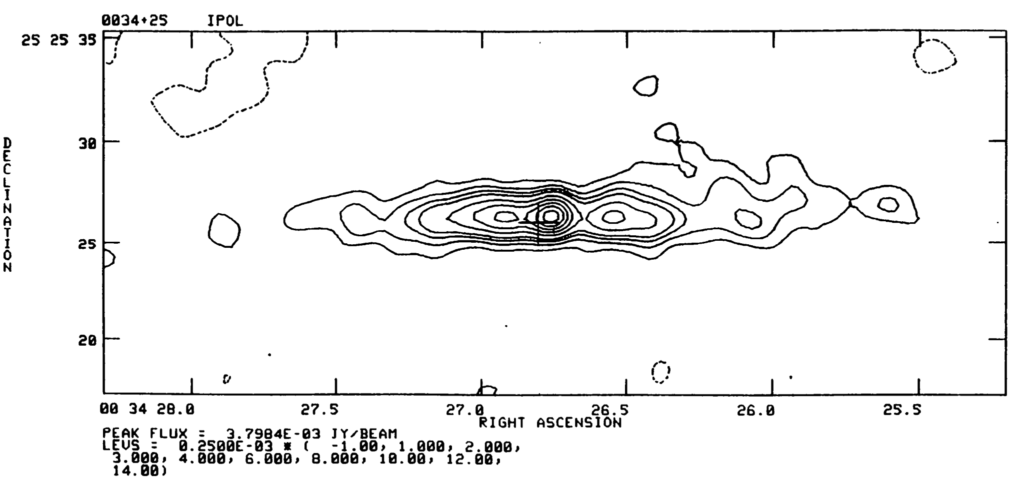

FIGURES 1-32. — Contour maps and radio photographs for sources of the « bright sample » (see text). Maps obtained combining the present observations with those made with the B array (Paper I) or the C array (Paper II) are distinguished by the letter AB and AC respectively. The cross marks the position of the optical identification.

FIGURES 33-72. — Same as figures 1-32, but for the « faint » sample.

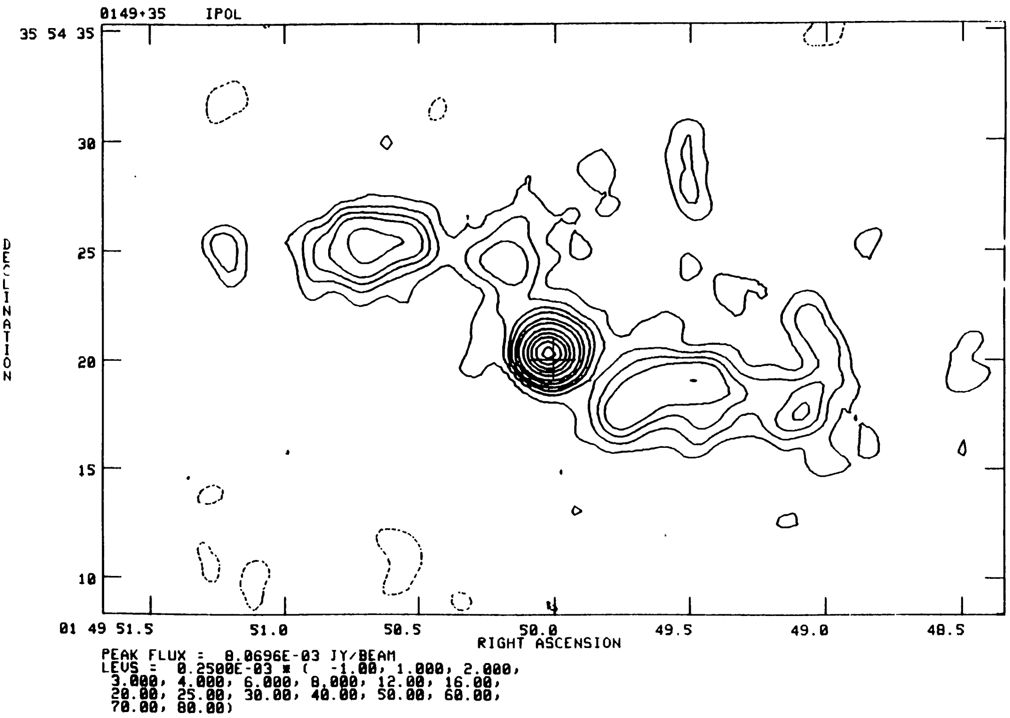

FIGURE 2.

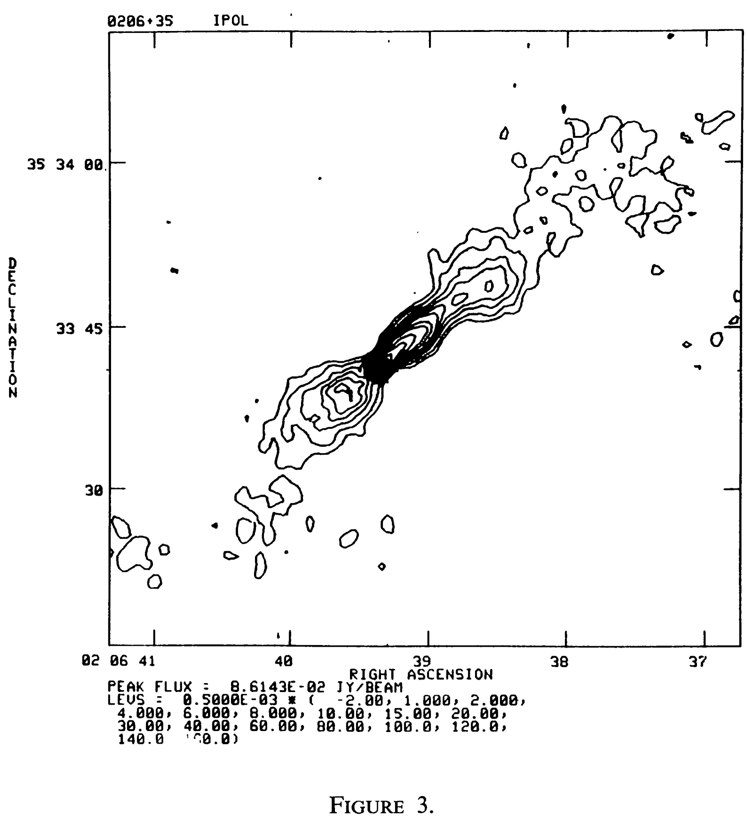

FIGURE 3.

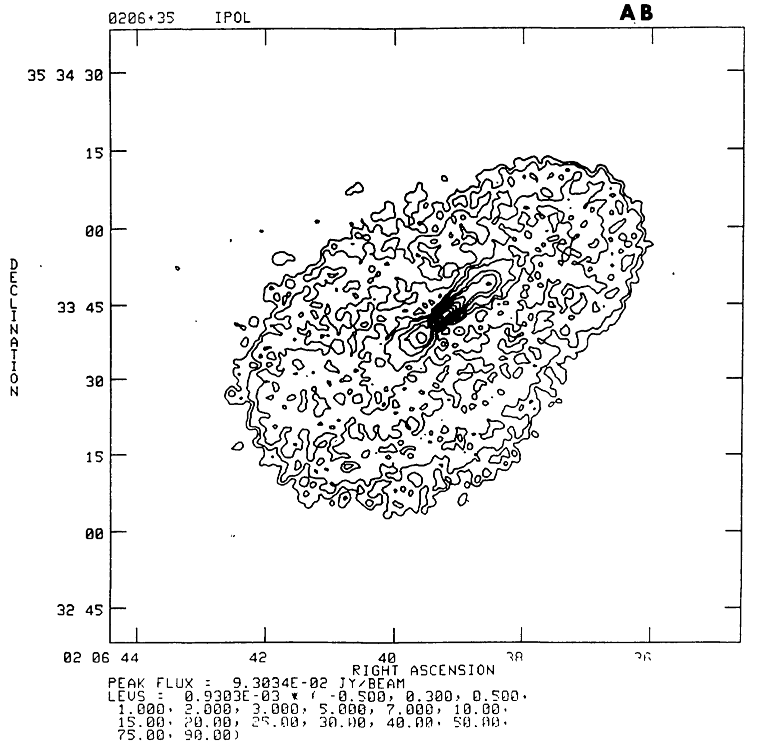

FIGURE 4.

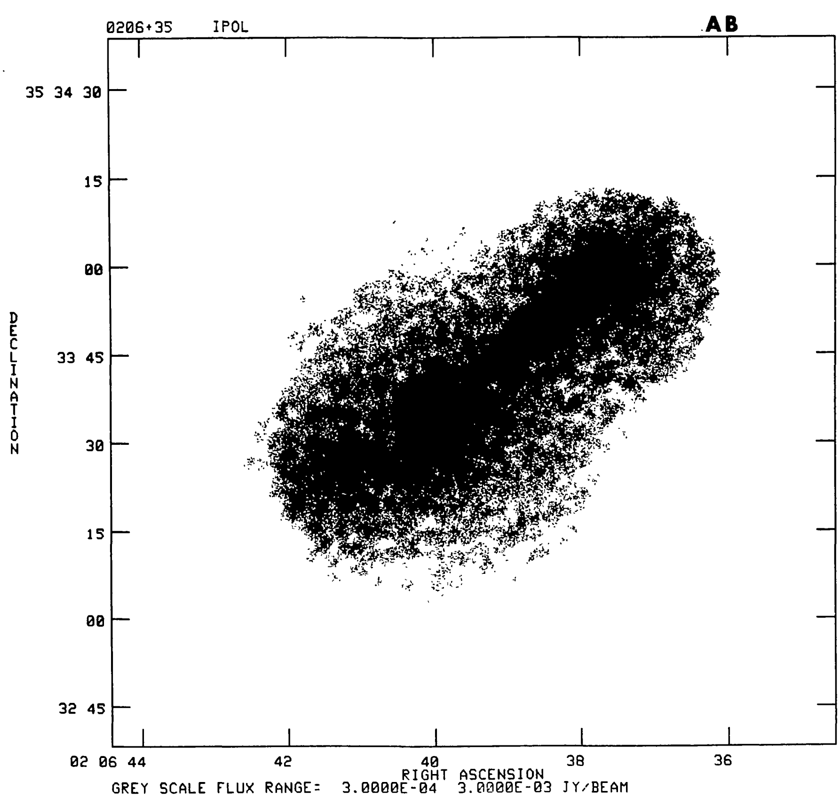

FIGURE 5.

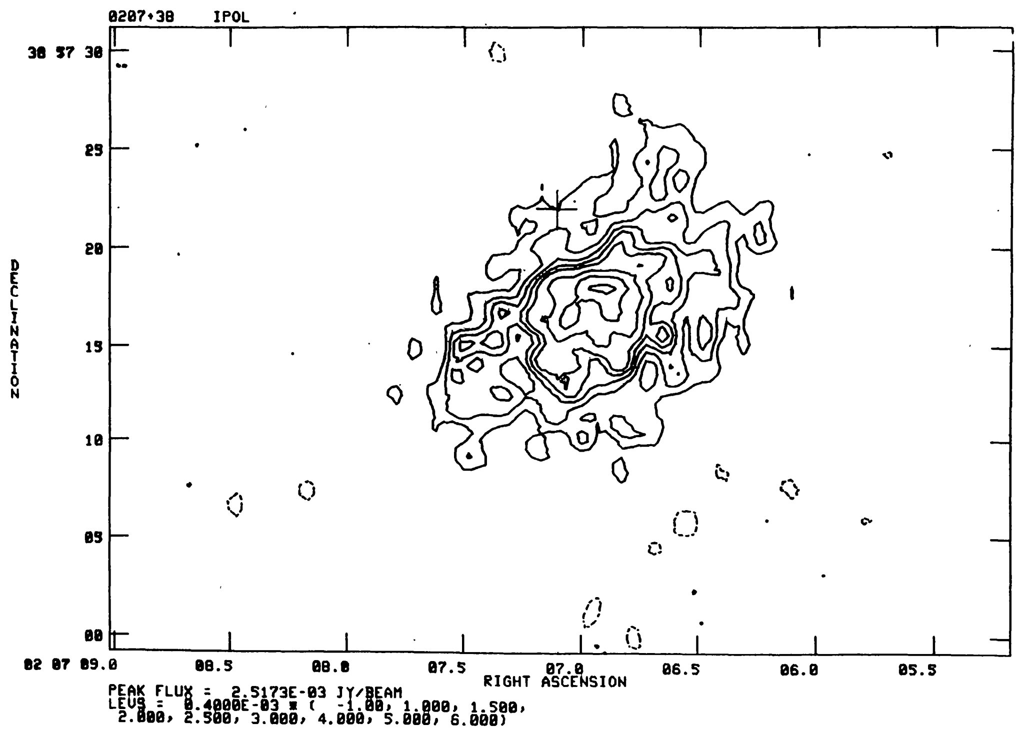

FIGURE 6.

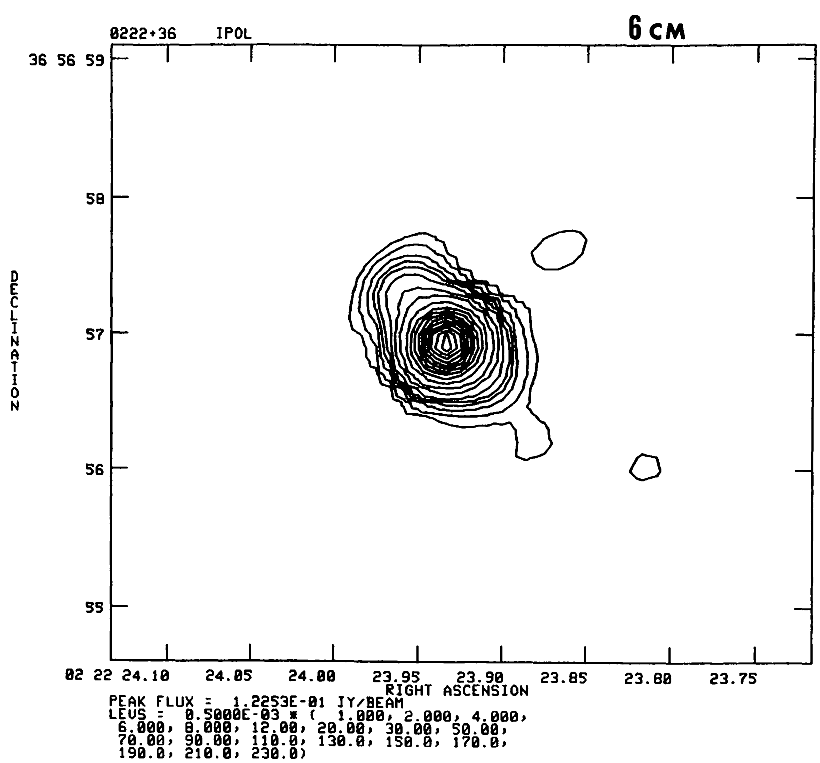

FIGURE 7.

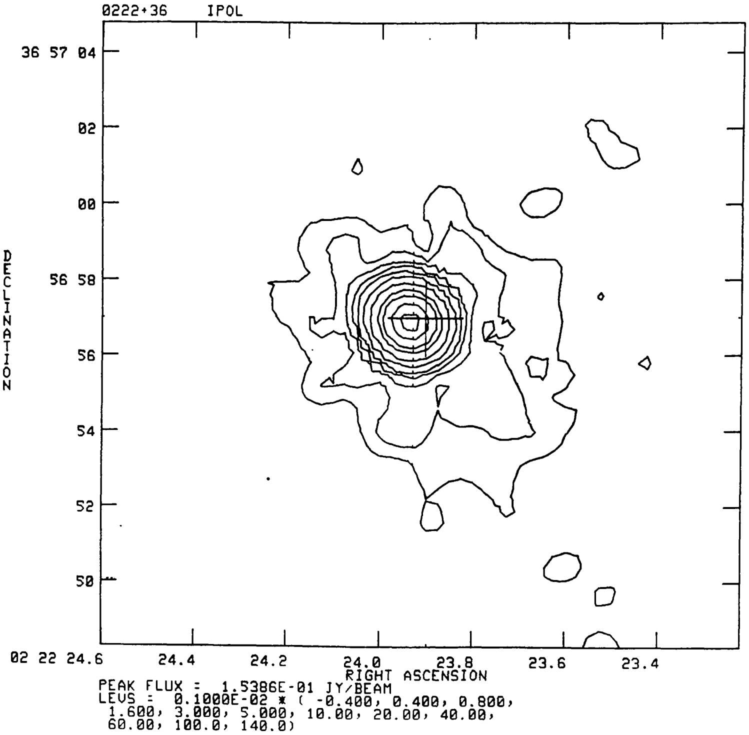

FIGURE 8.

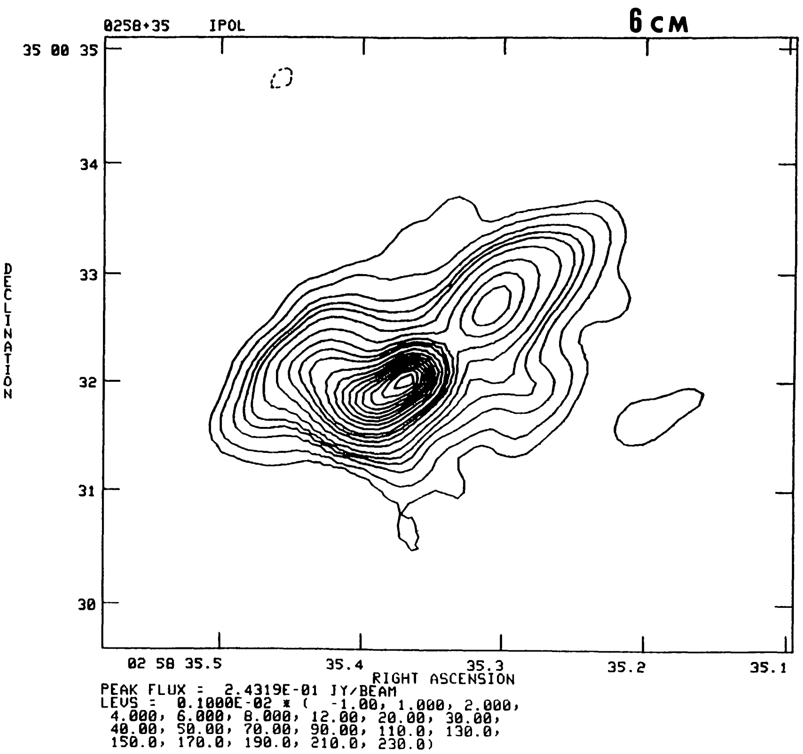

FIGURE 9.

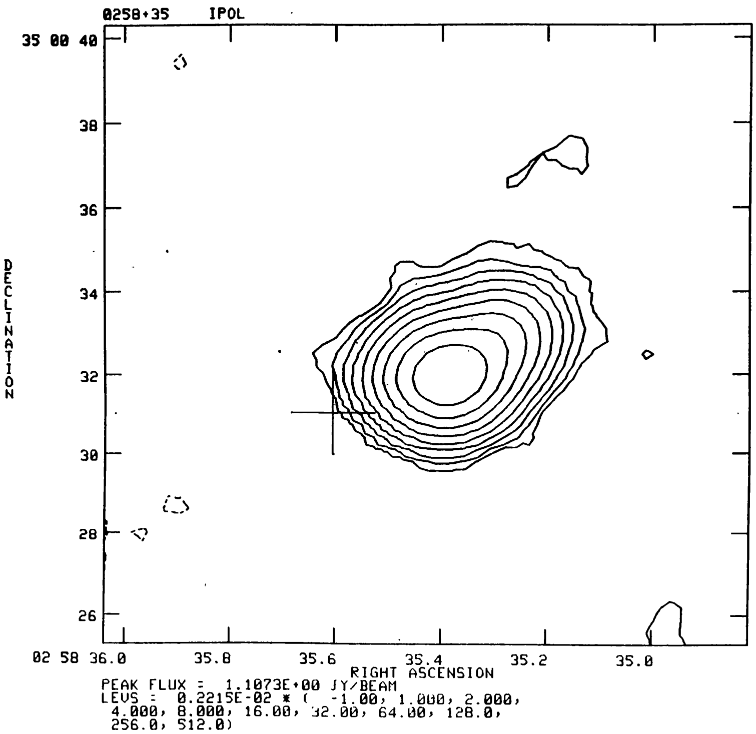

FIGURE 10.

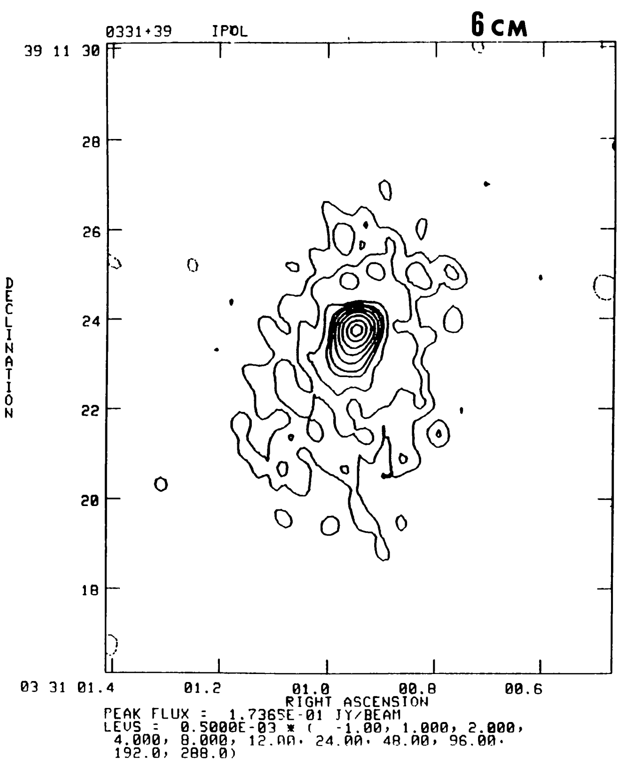

FIGURE 11.

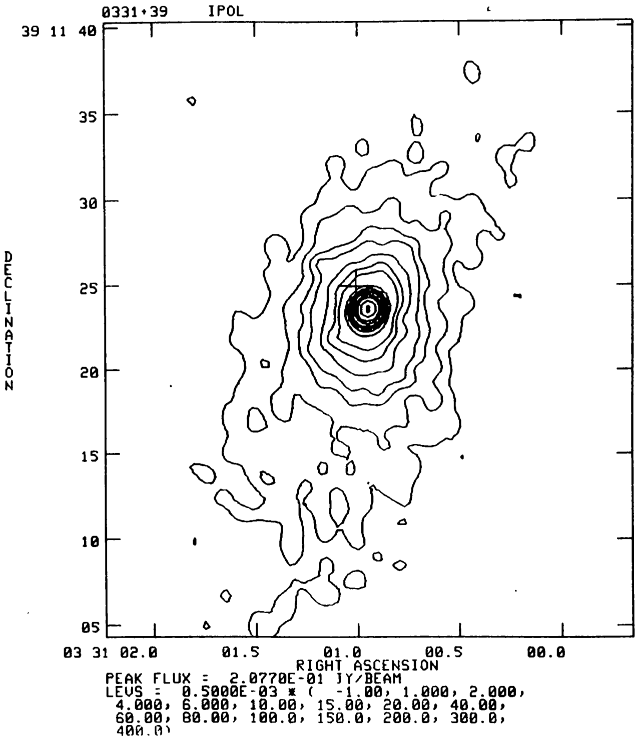

FIGURE 12.

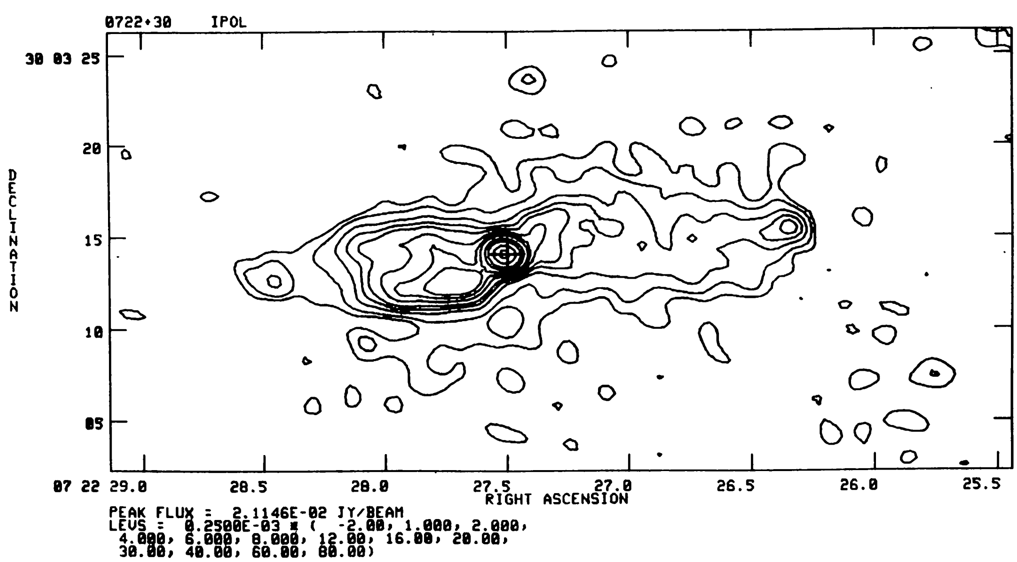

FIGURE 13.

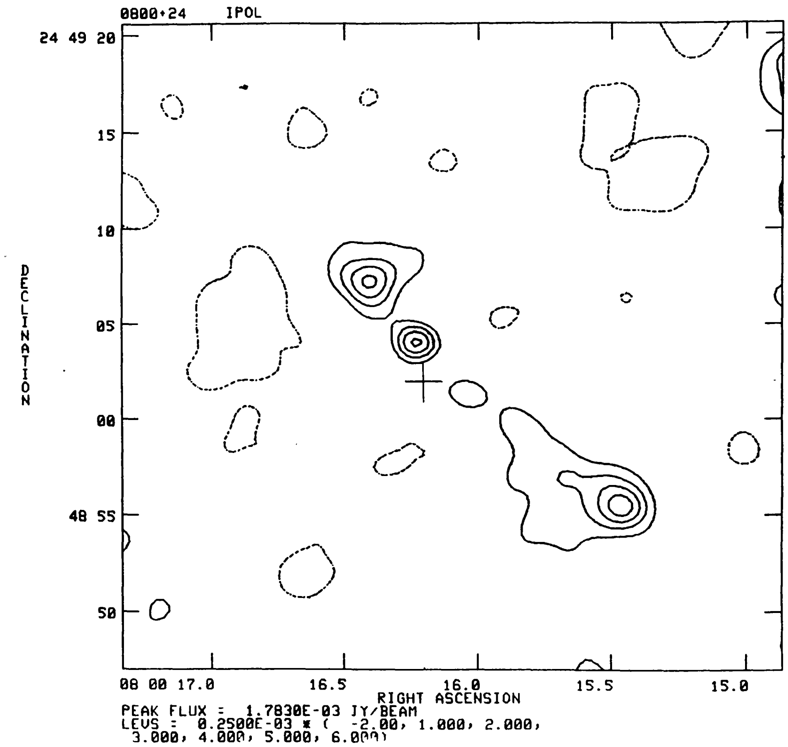

FIGURE 14.

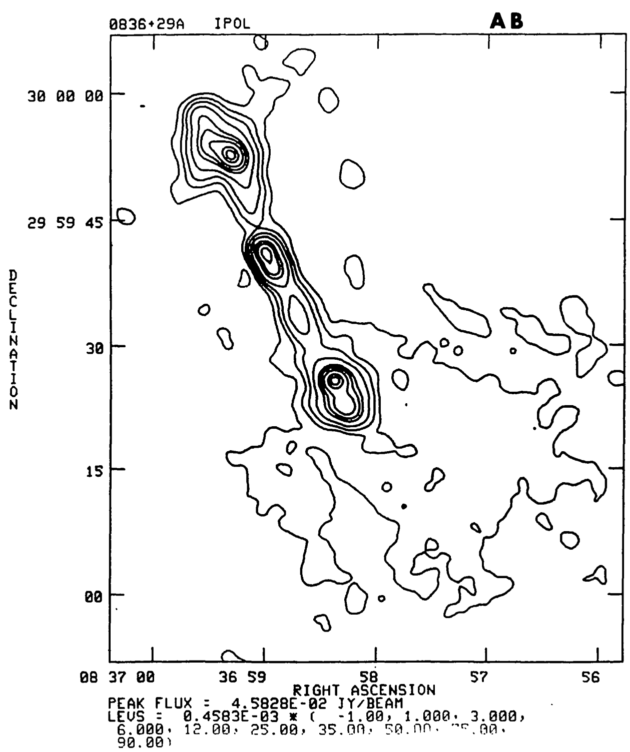

FIGURE 15.

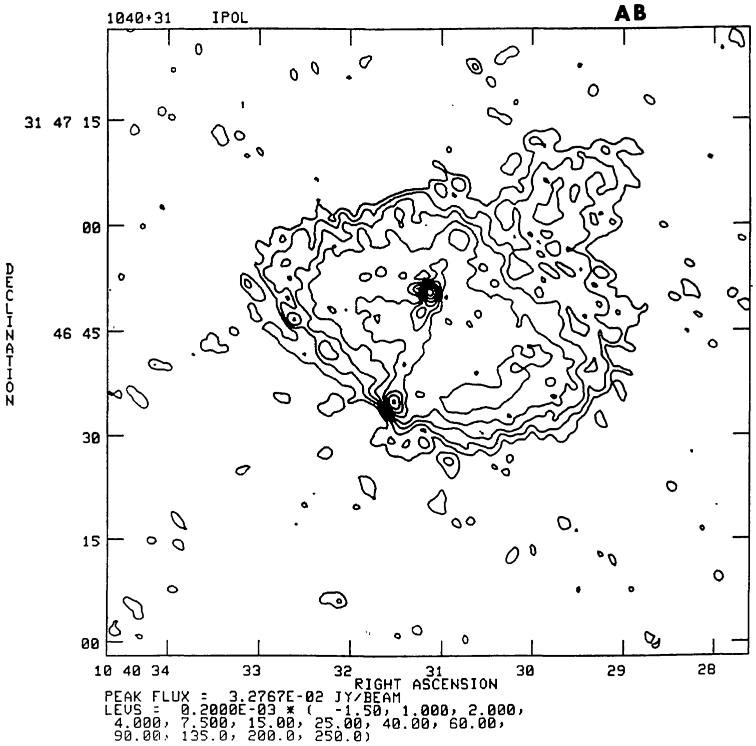

FIGURE 16.

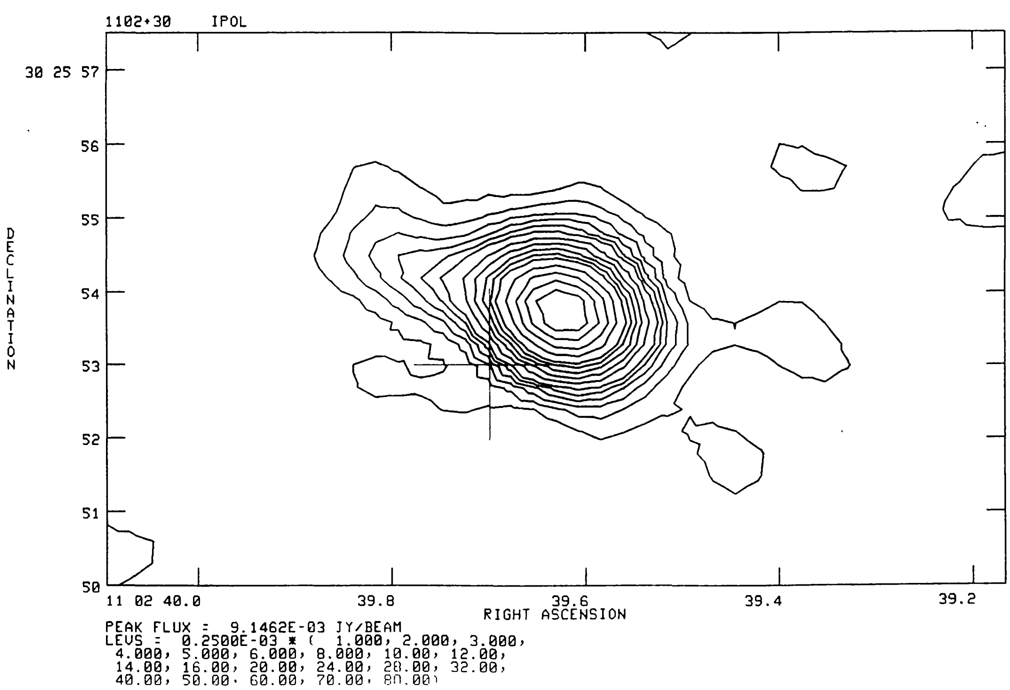

FIGURE 17.

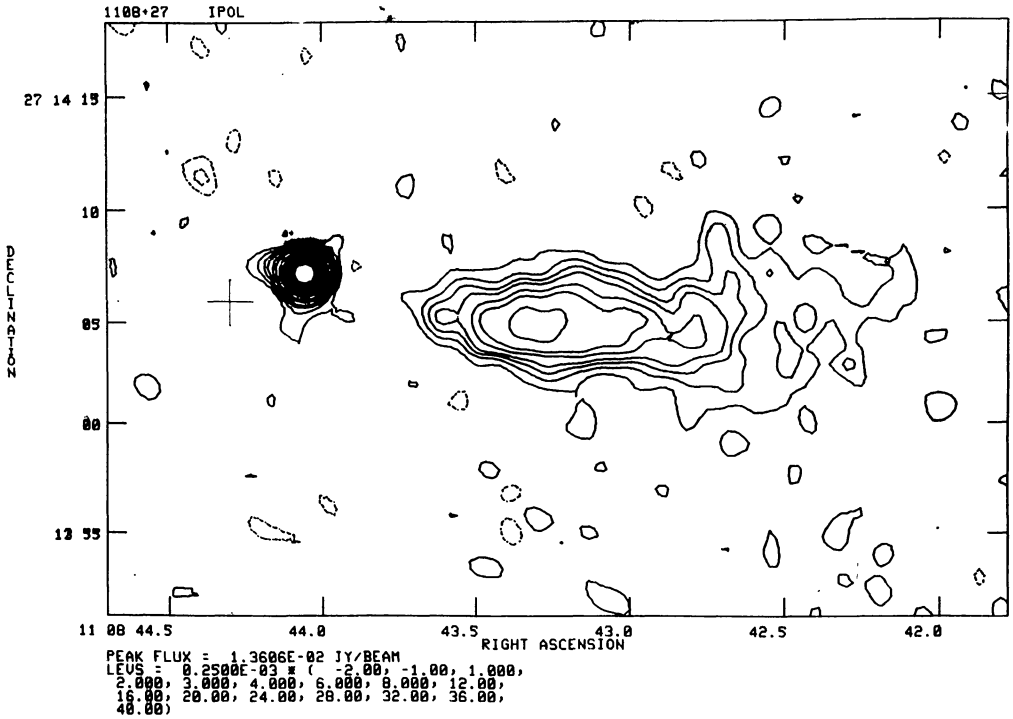

FIGURE 18.

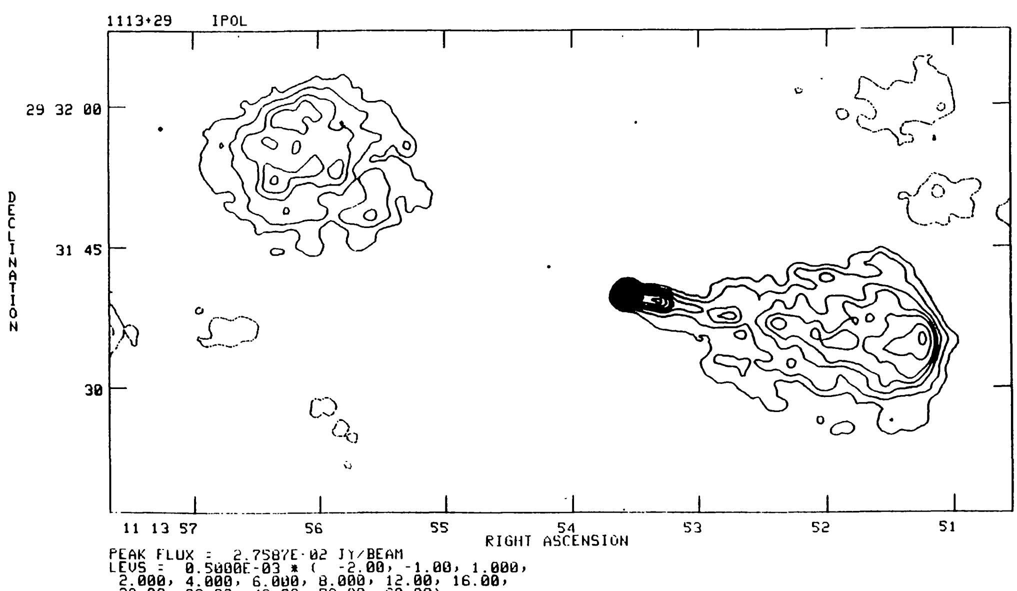

FIGURE 19.

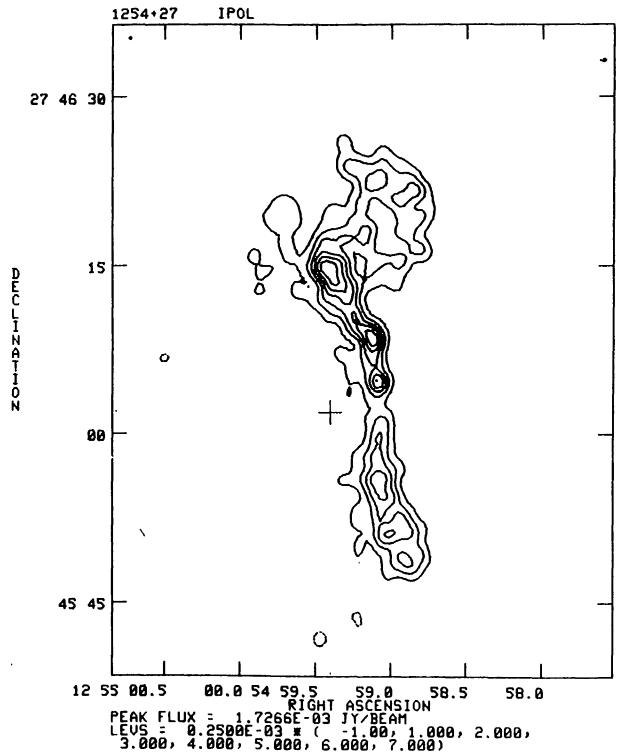

FIGURE 20.

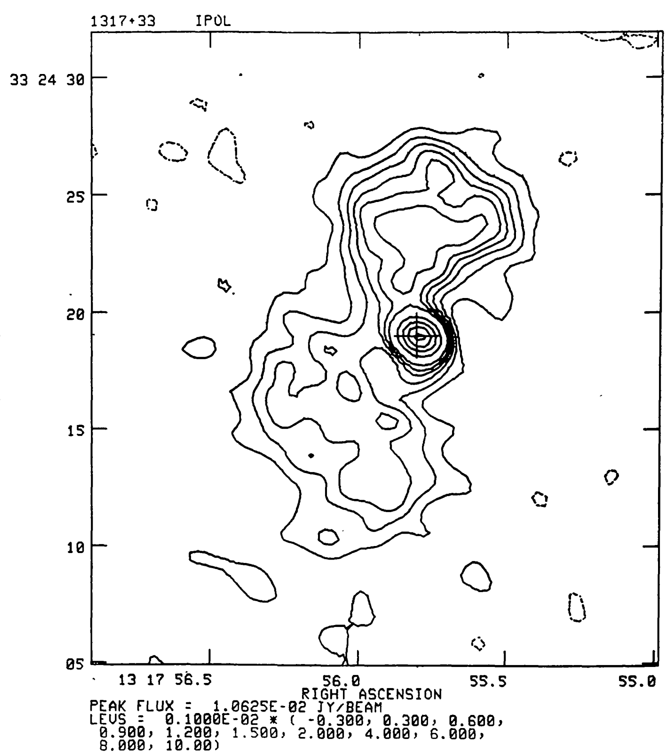

FIGURE 21.

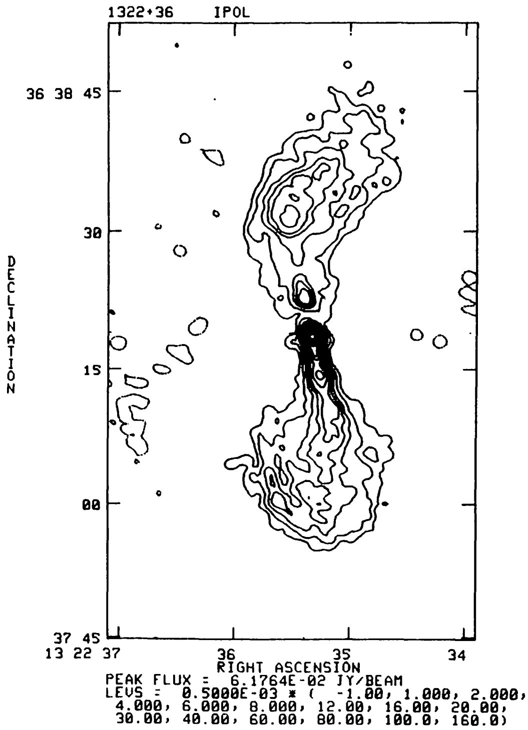

FIGURE 22.

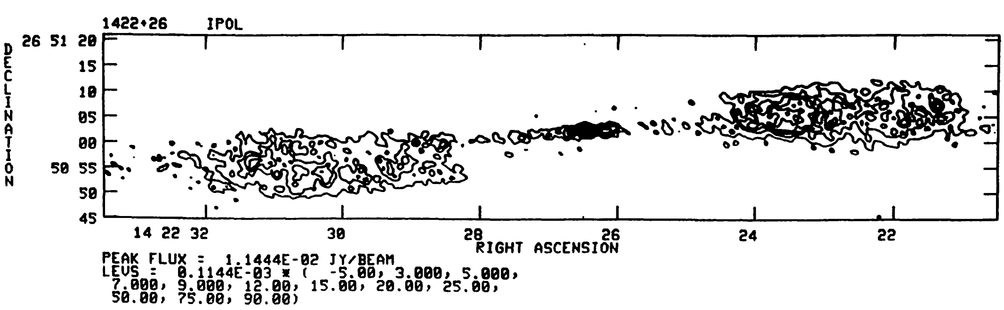

FIGURE 23.

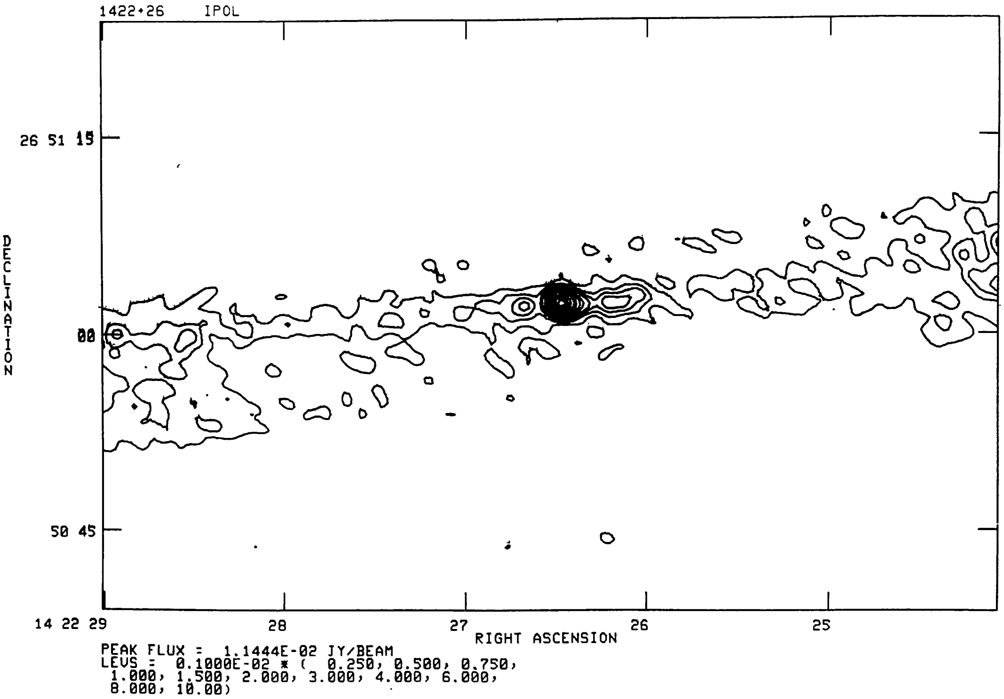

FIGURE 24.

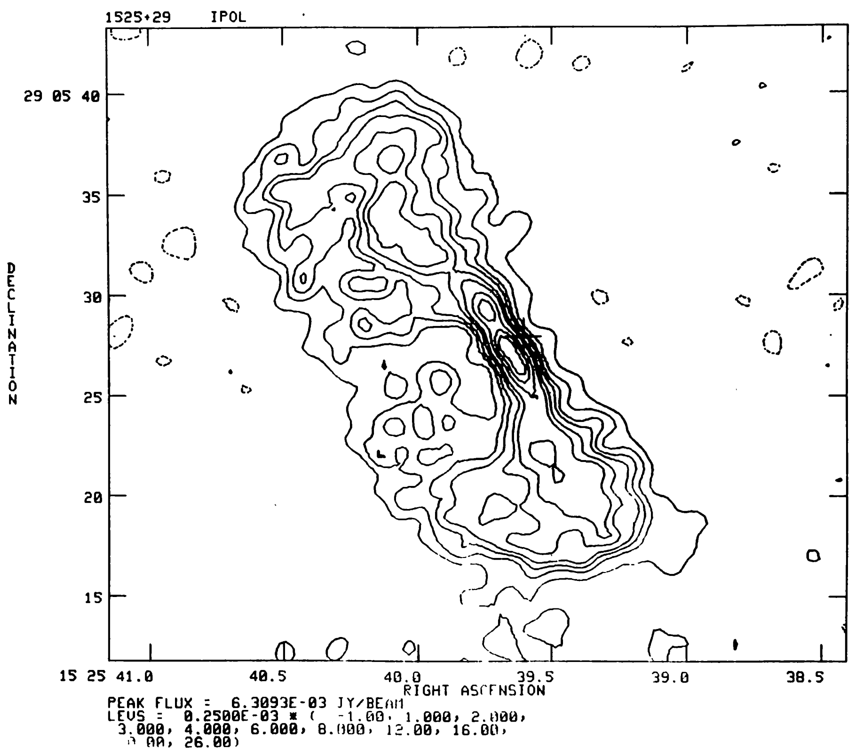

FIGURE 25.

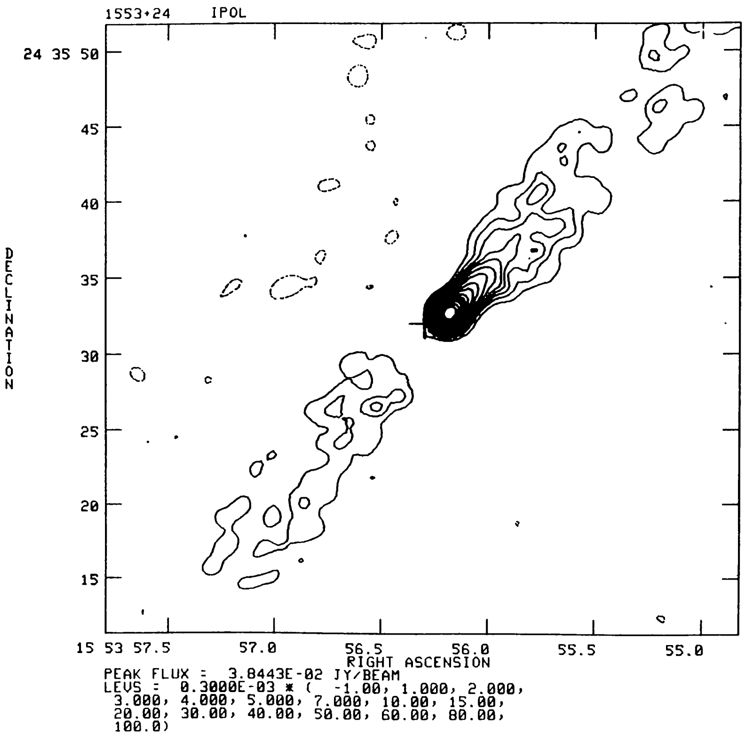

FIGURE 26.

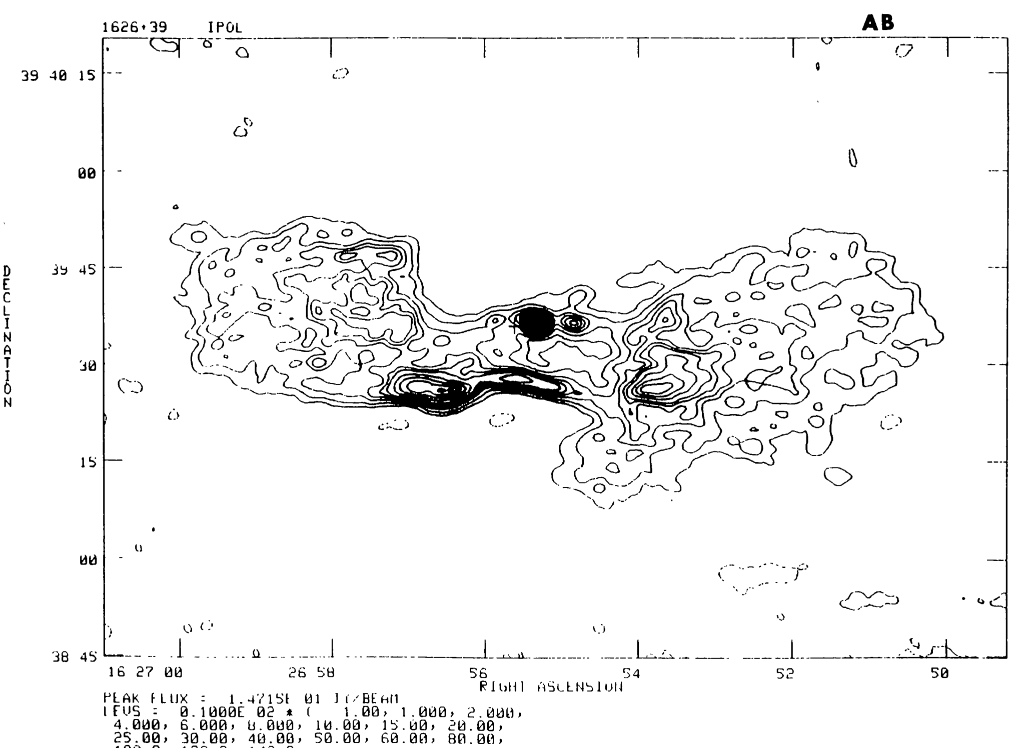

FIGURE 27.

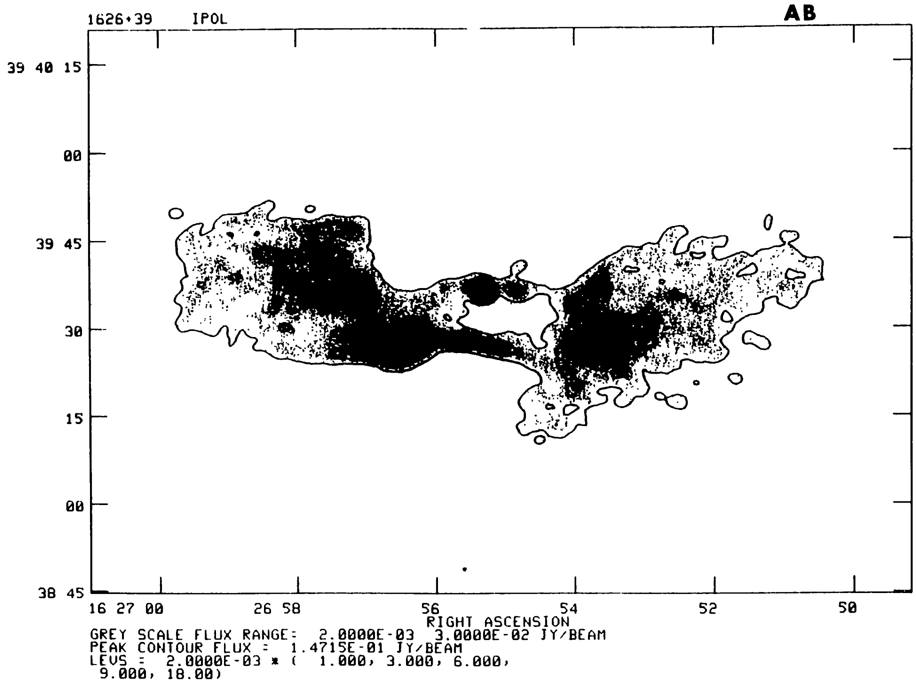

FIGURE 28.

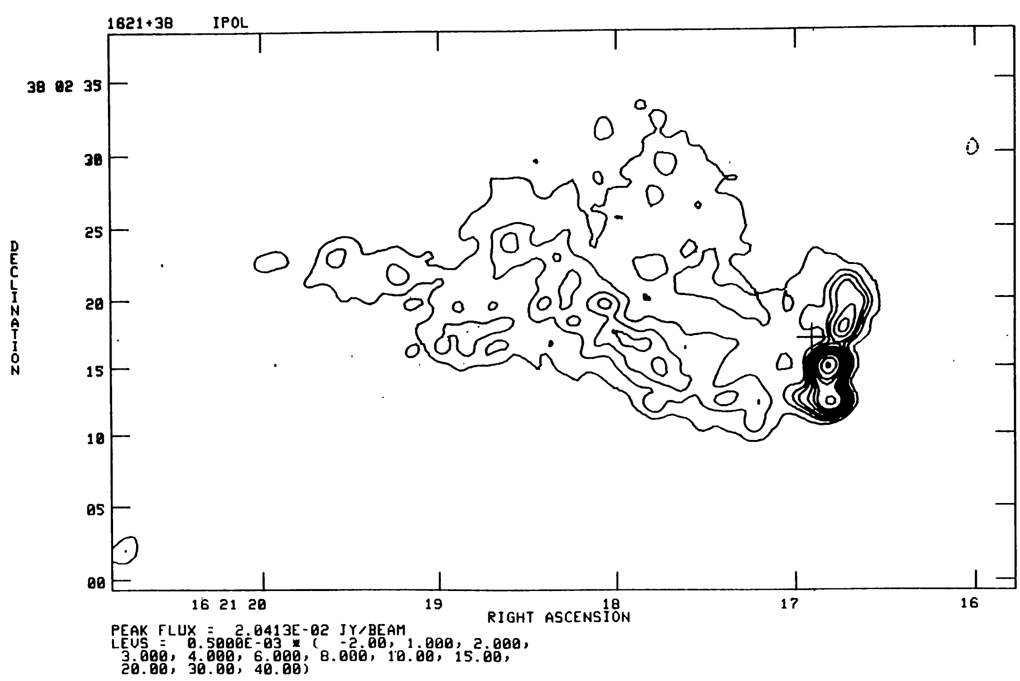

FIGURE 29.

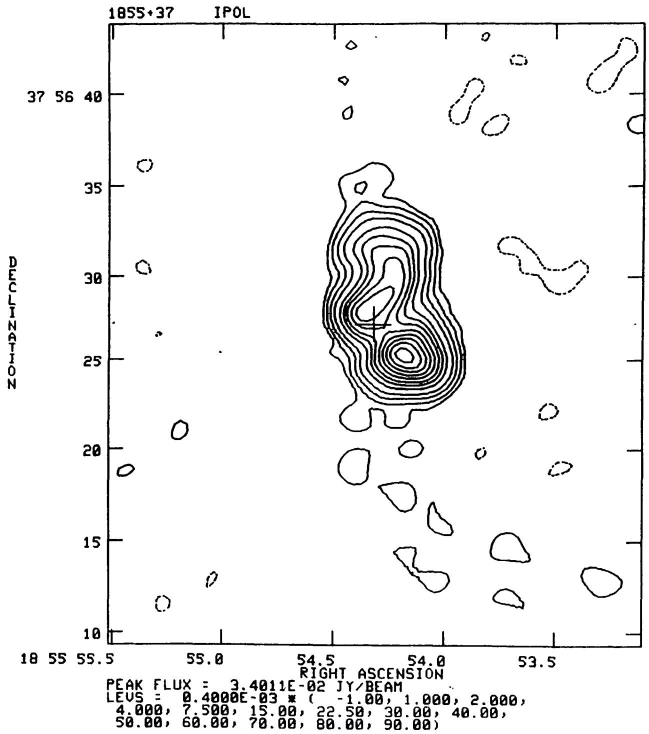

FIGURE 30.

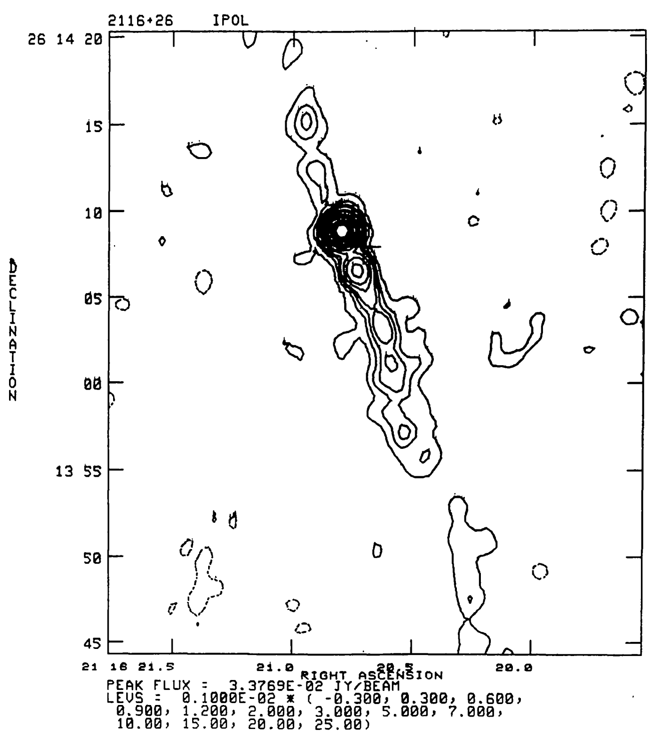

FIGURE 31.

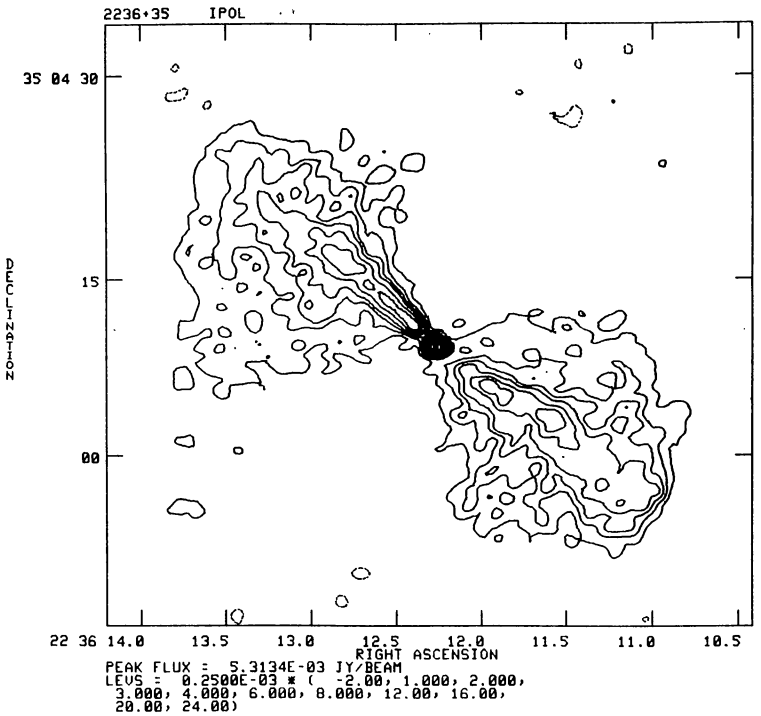

FIGURE 32.

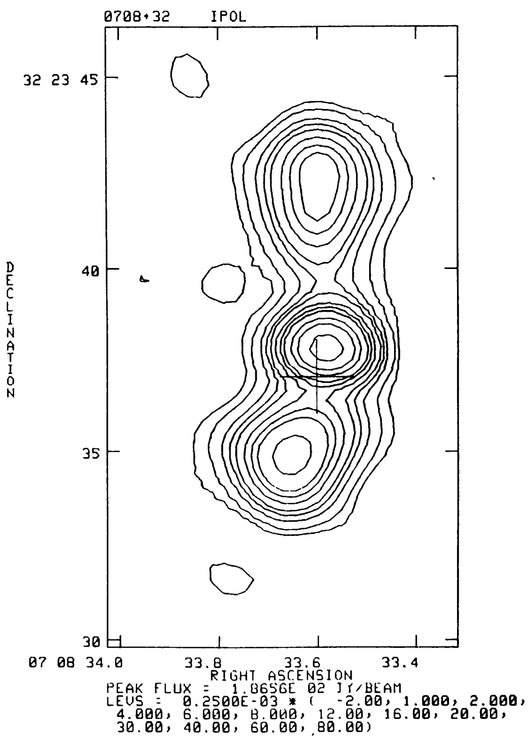

FIGURE 33.

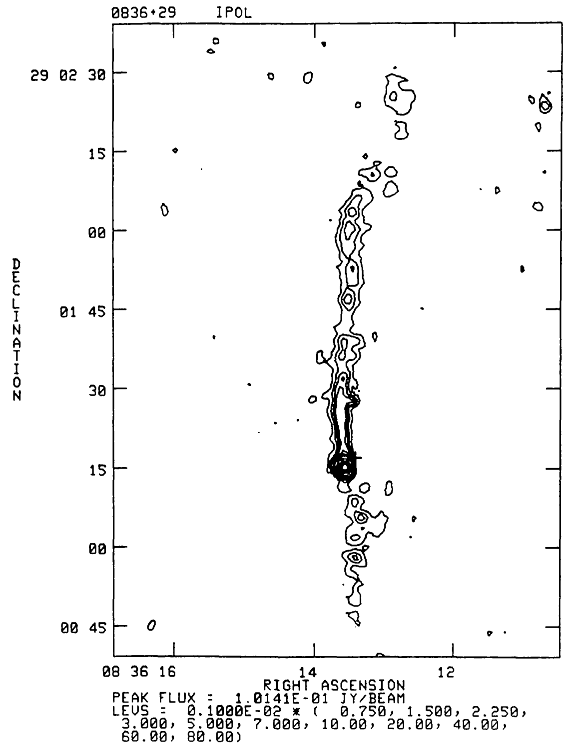

FIGURE 34.

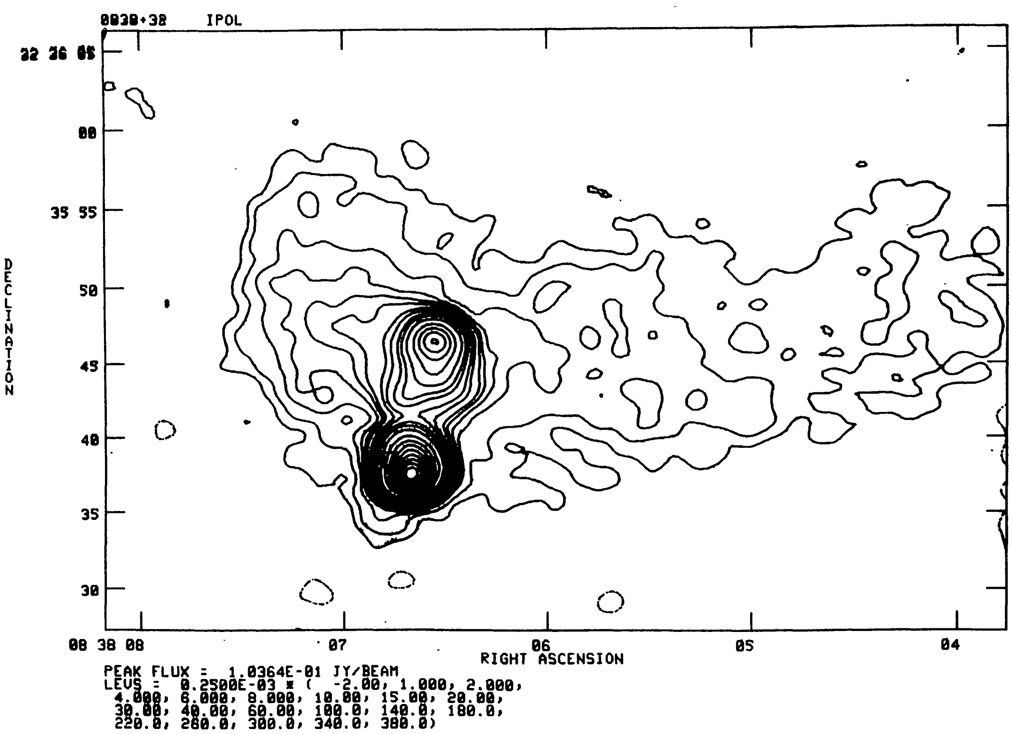

FIGURE 35.

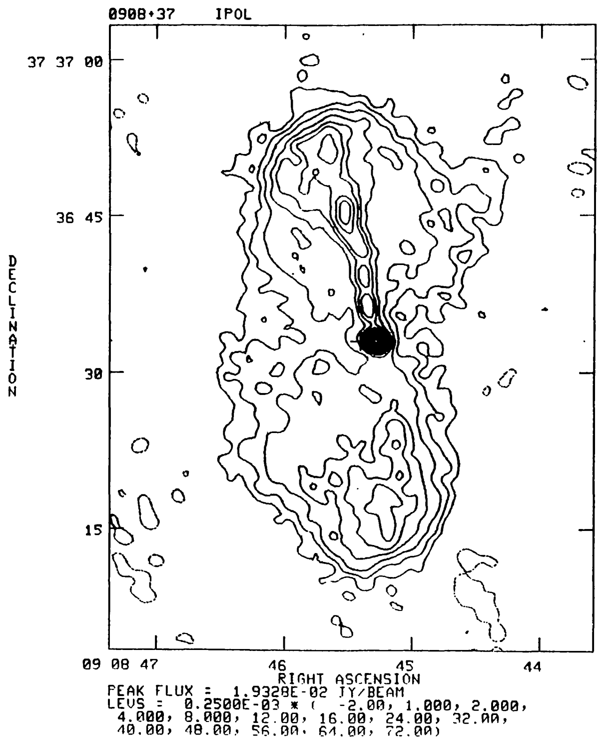

FIGURE 36.

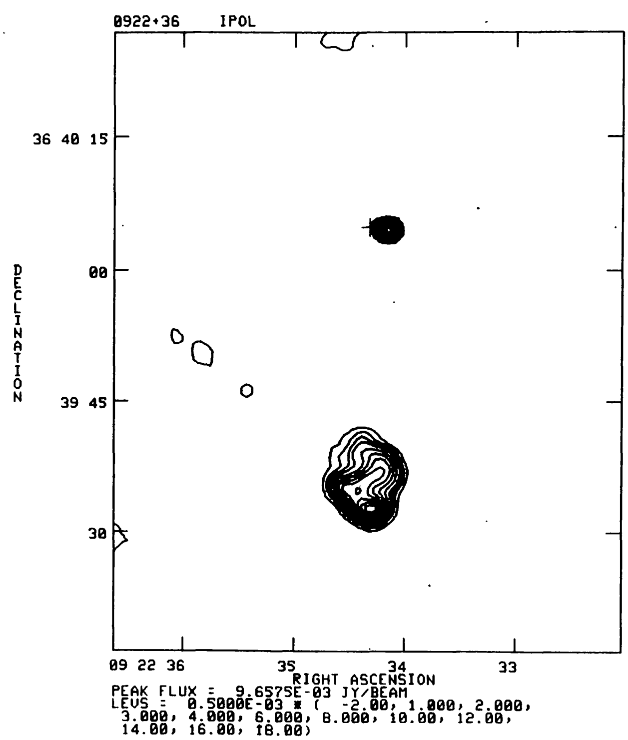

FIGURE 37.

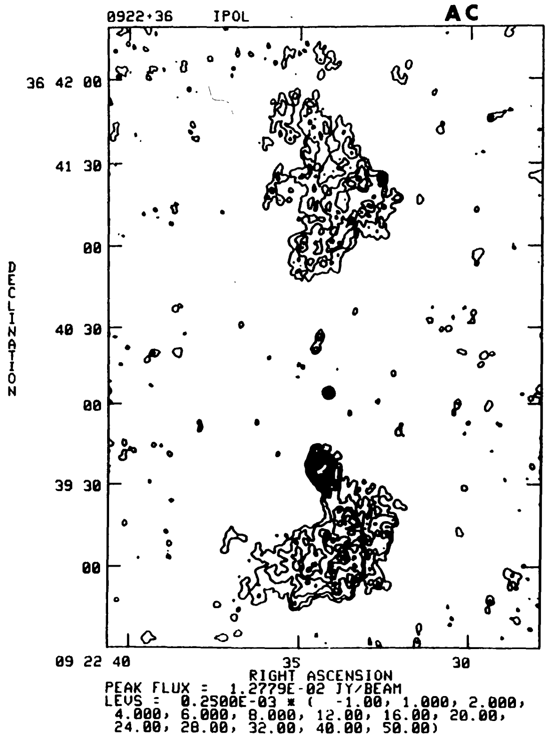

FIGURE 38.

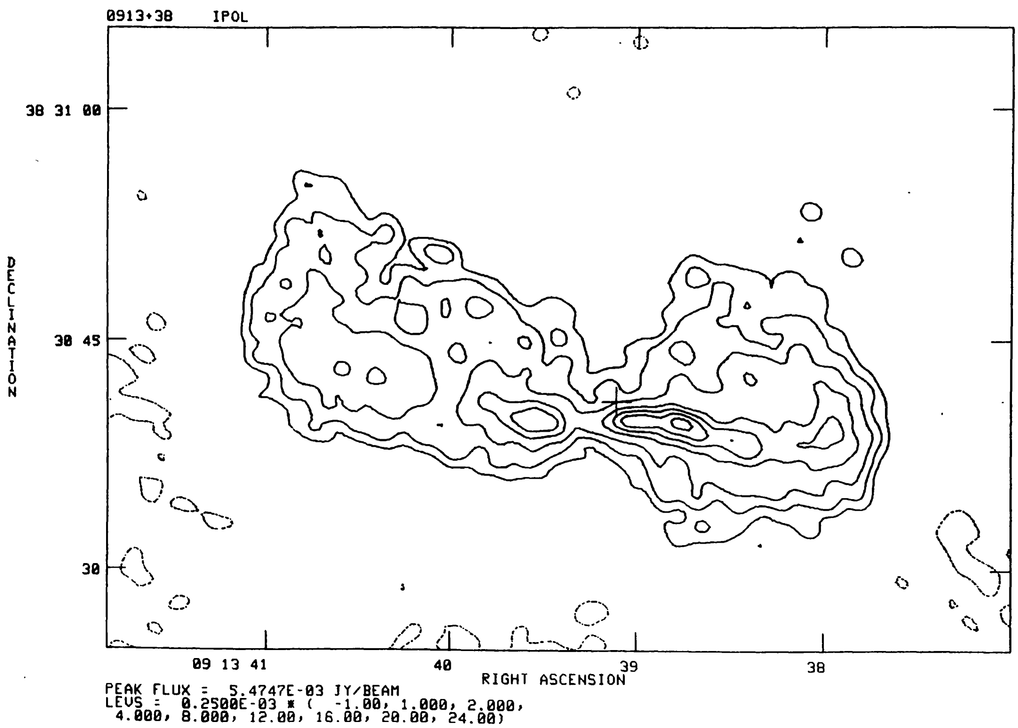

FIGURE 39.

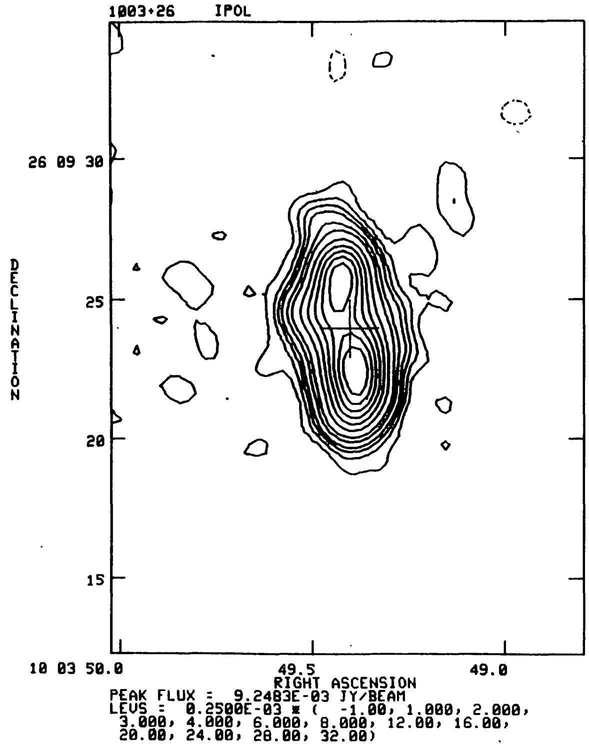

FIGURE 40.

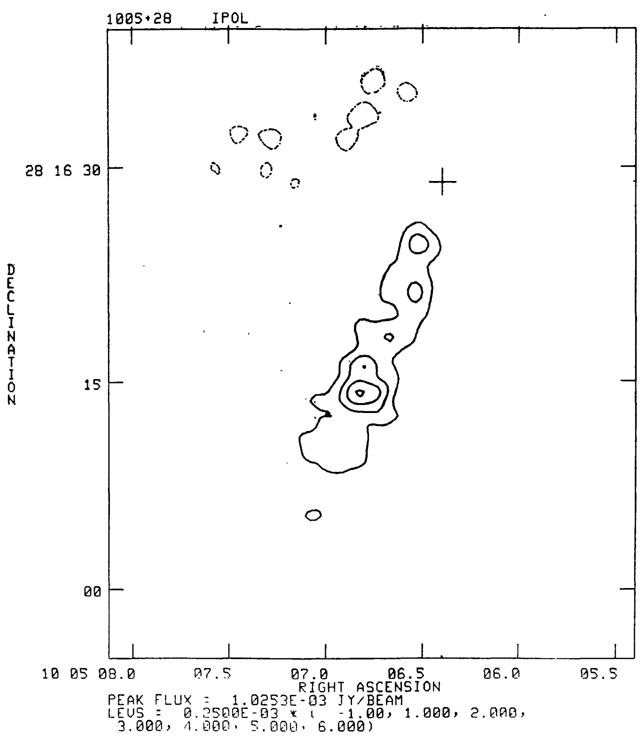

FIGURE 41.

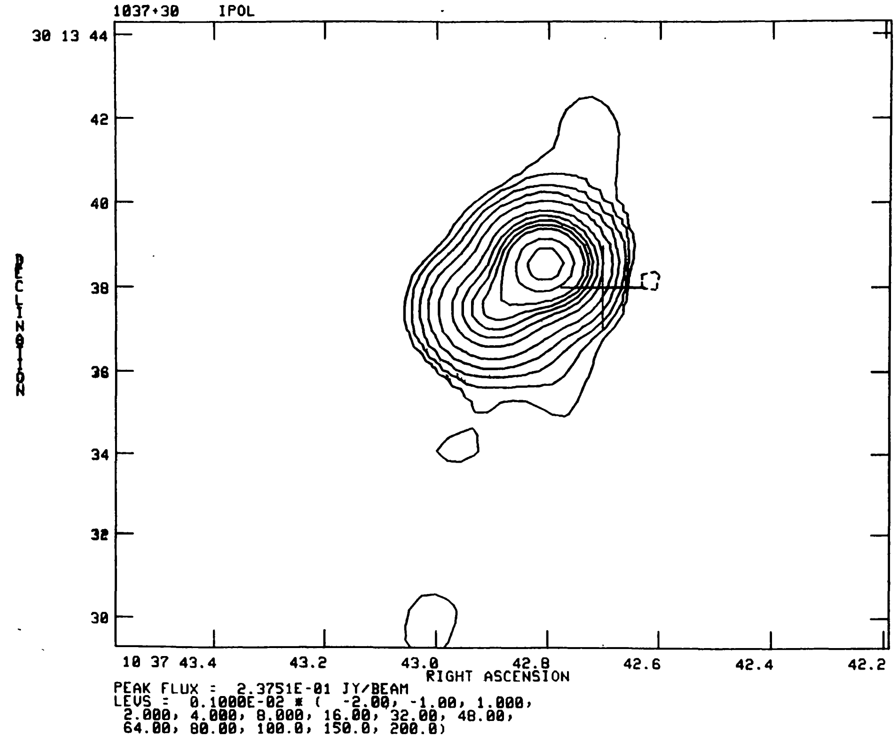

FIGURE 42.

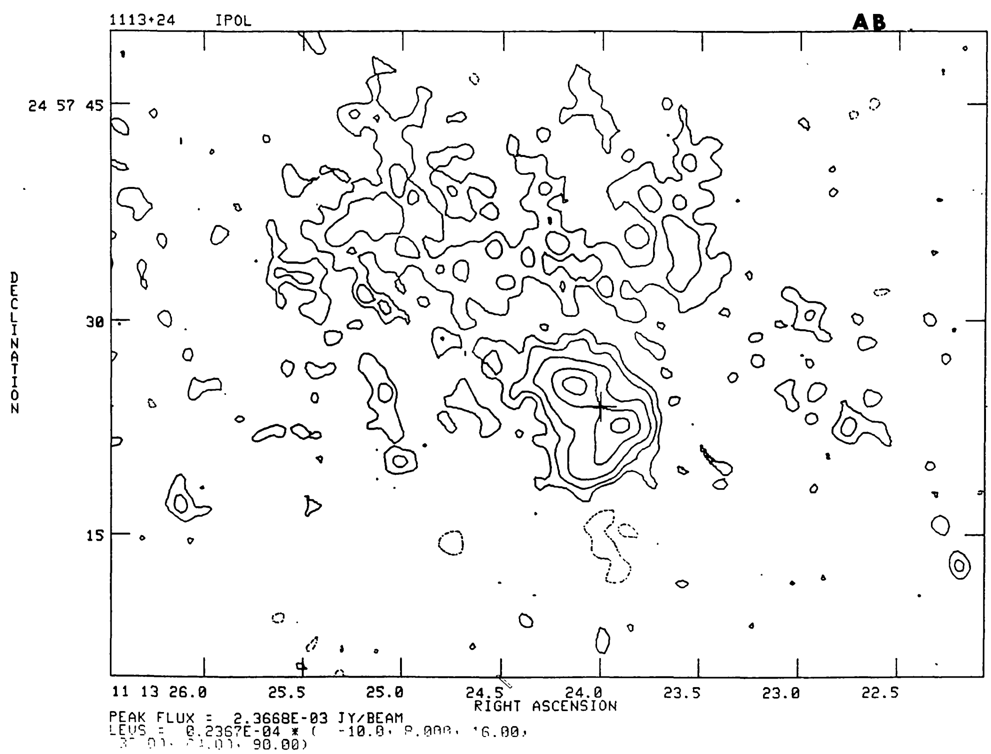

FIGURE 43.

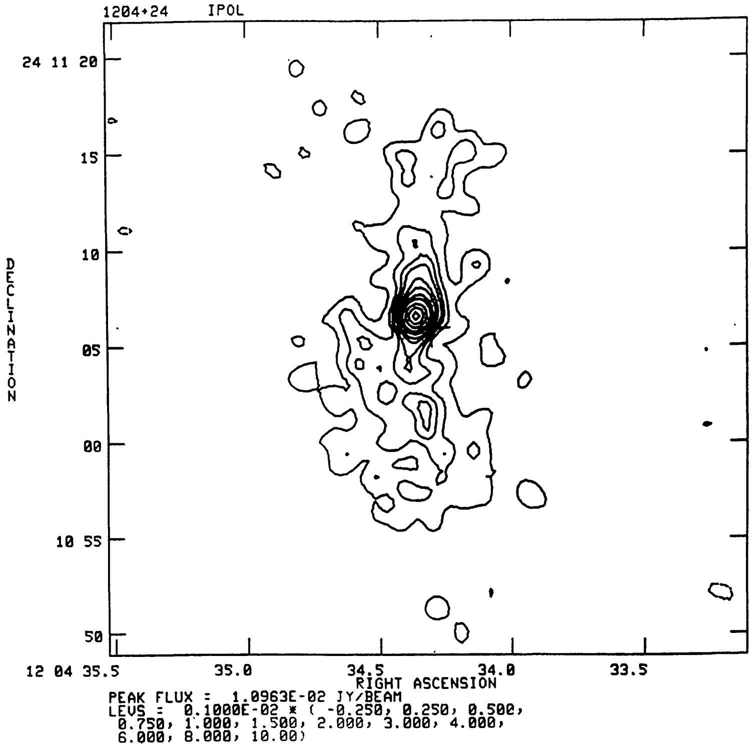

FIGURE 44.

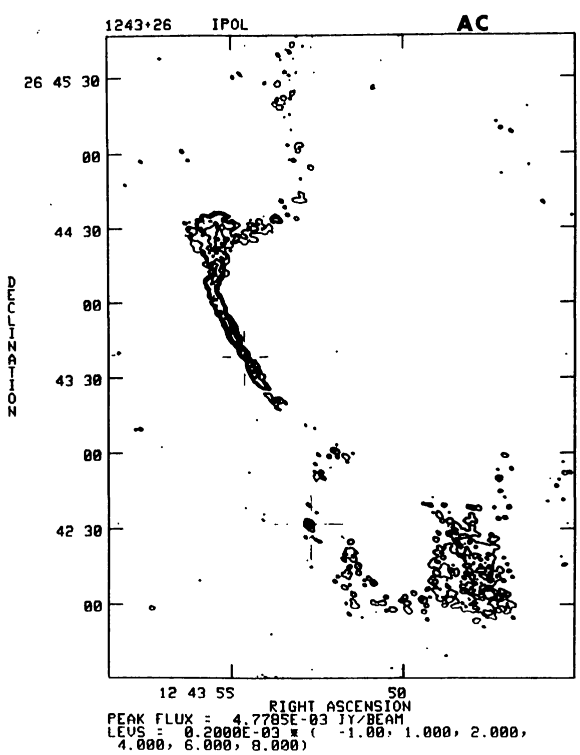

FIGURE 45.

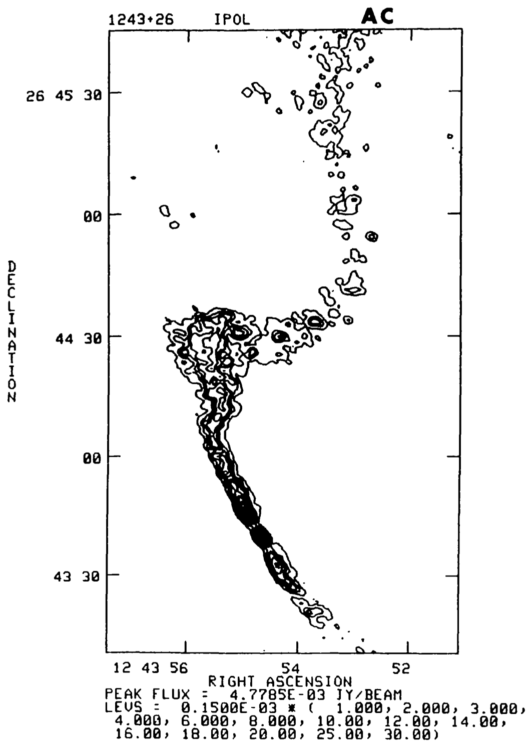

FIGURE 46.

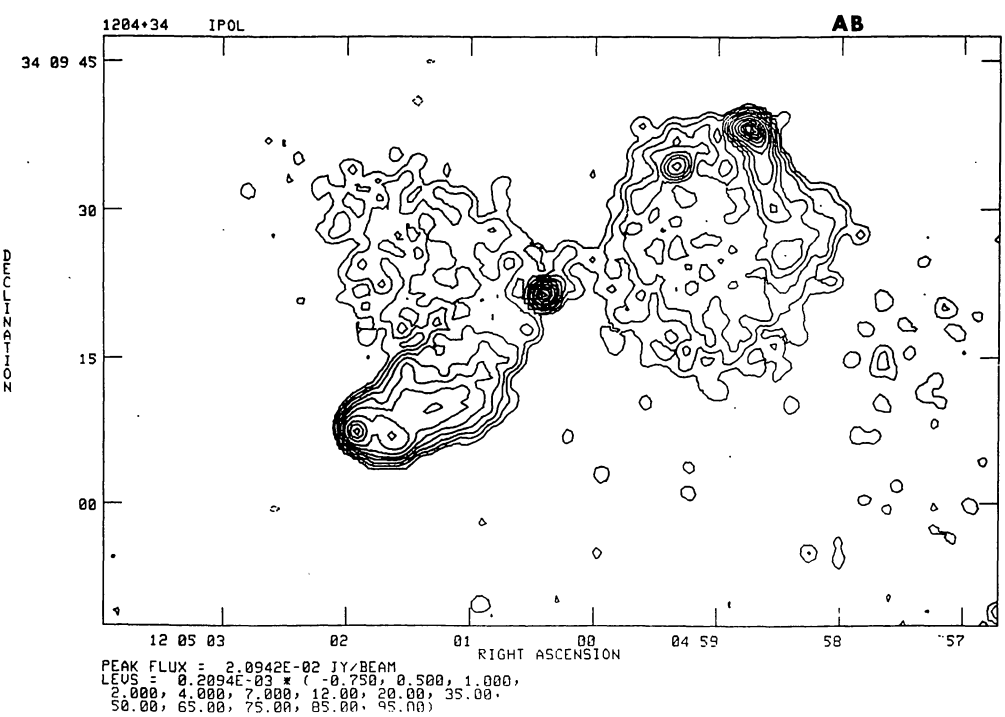

FIGURE 47.

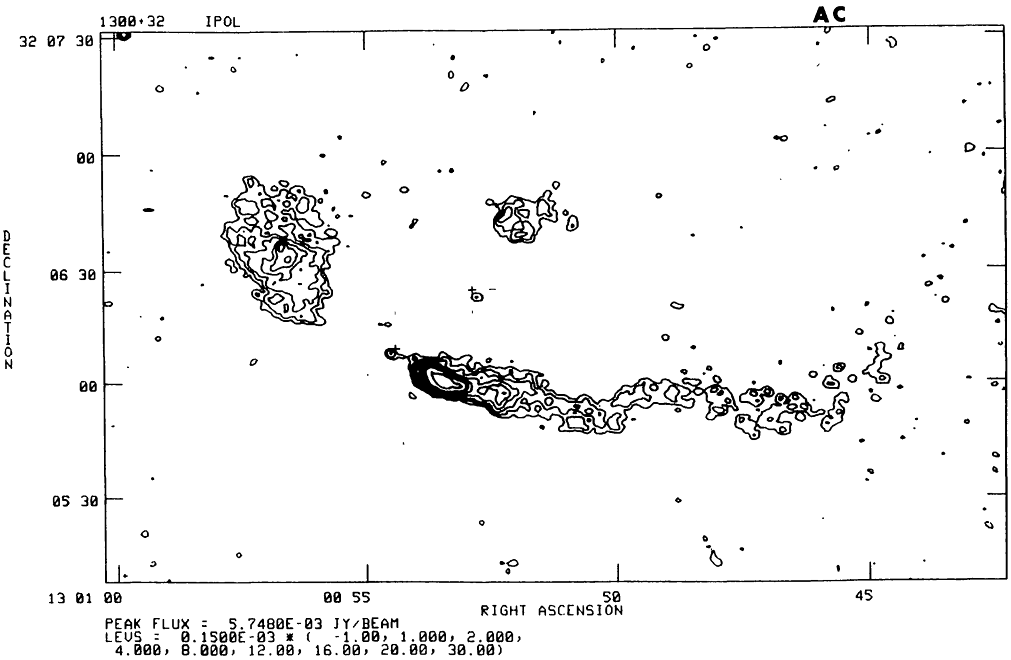

FIGURE 48.

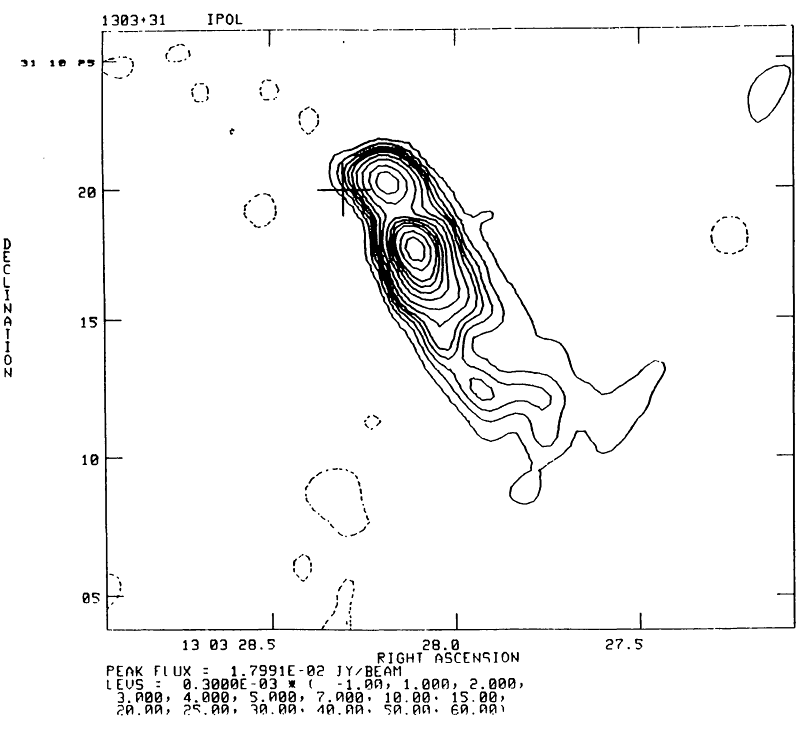

FIGURE 49.

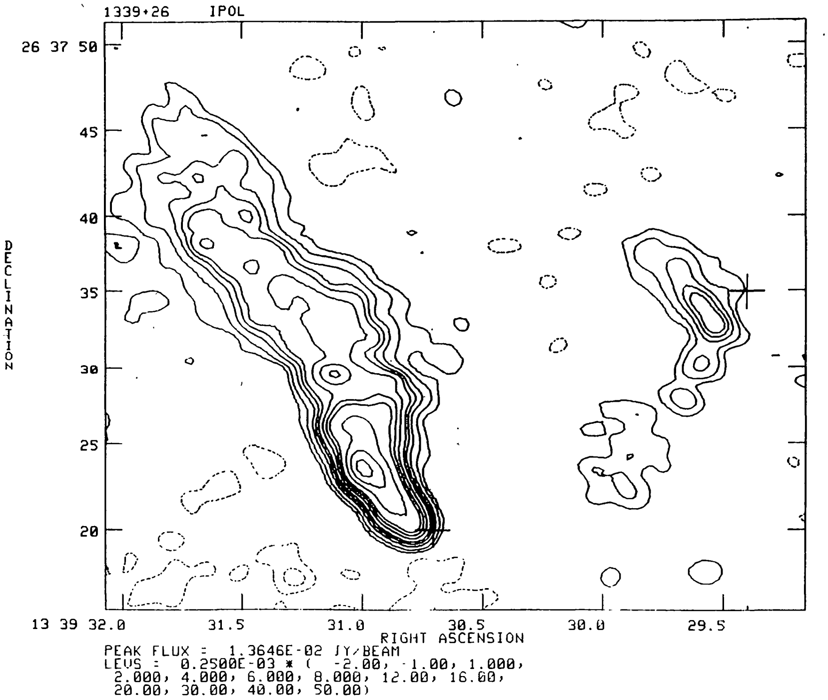

FIGURE 50.

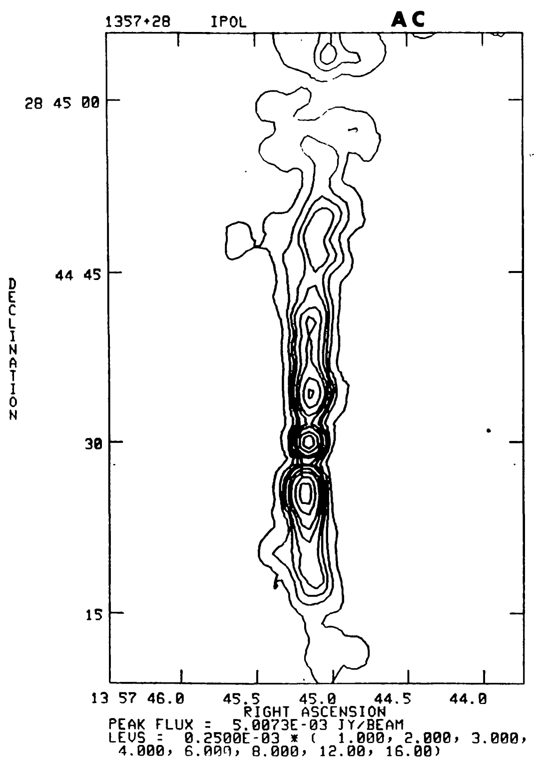

FIGURE 51.

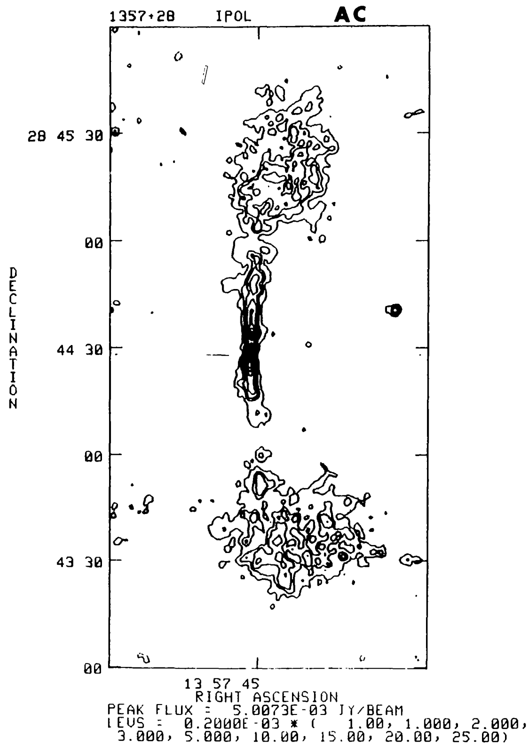

FIGURE 52.

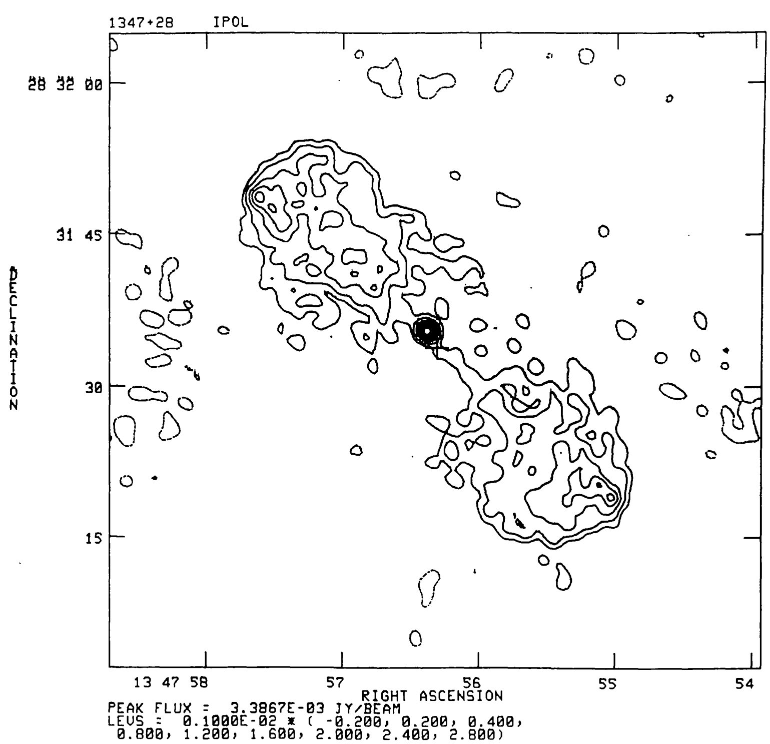

FIGURE 53.

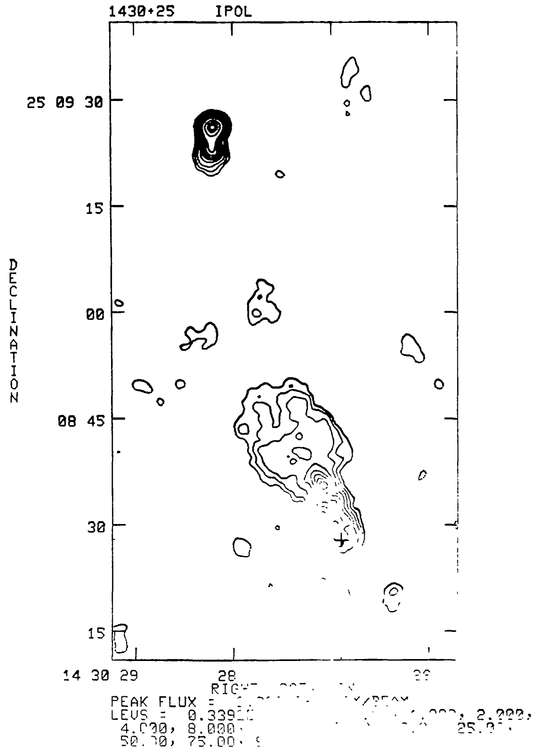

FIGURE 54.

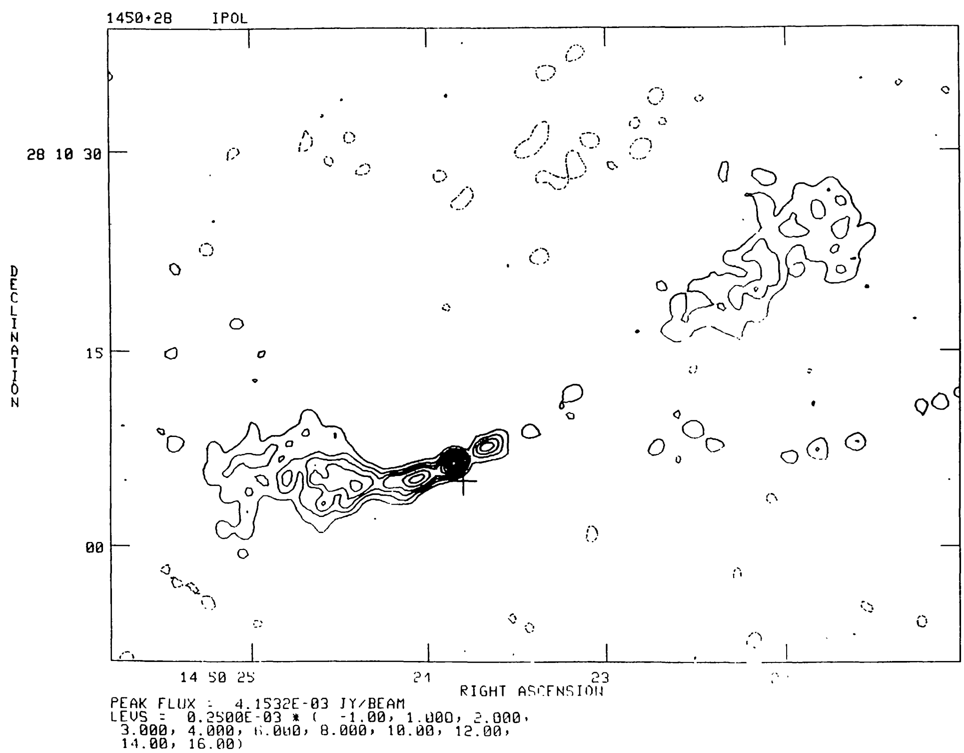

FIGURE 55.

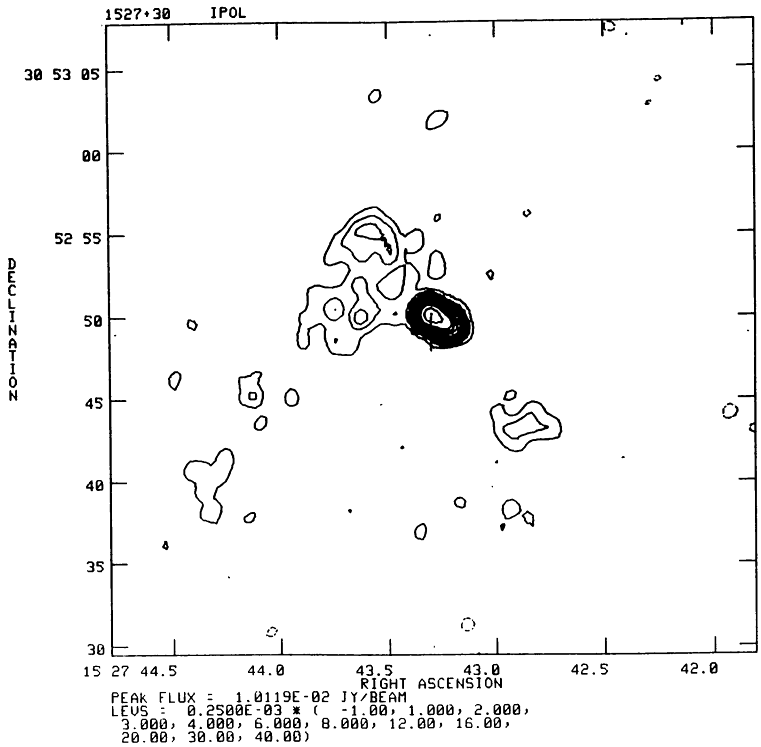

FIGURE 56.

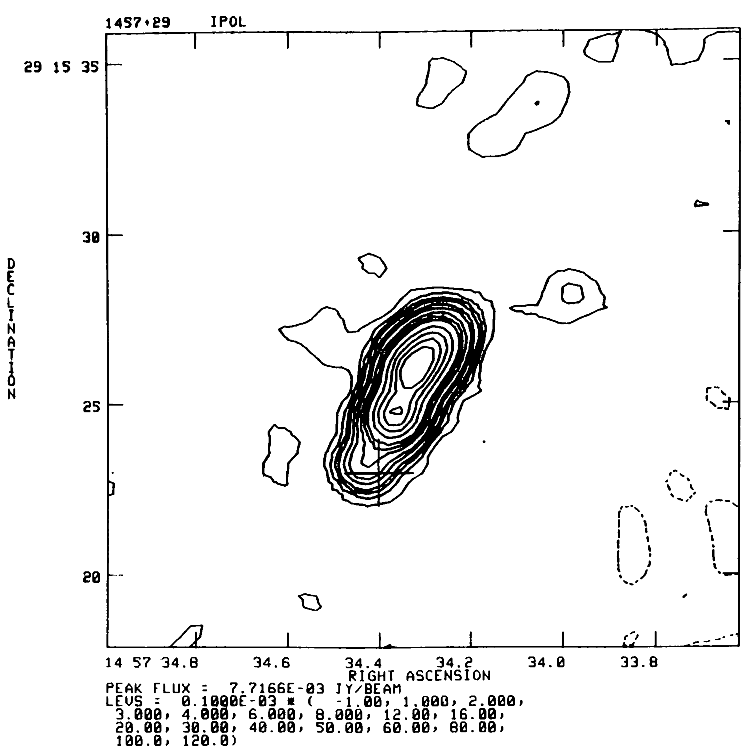

FIGURE 57.

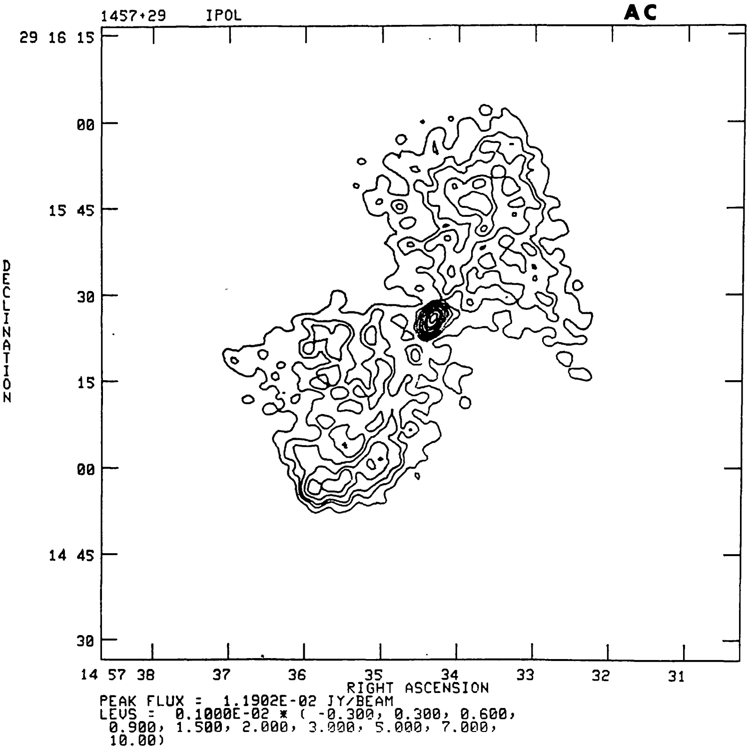

FIGURE 58.

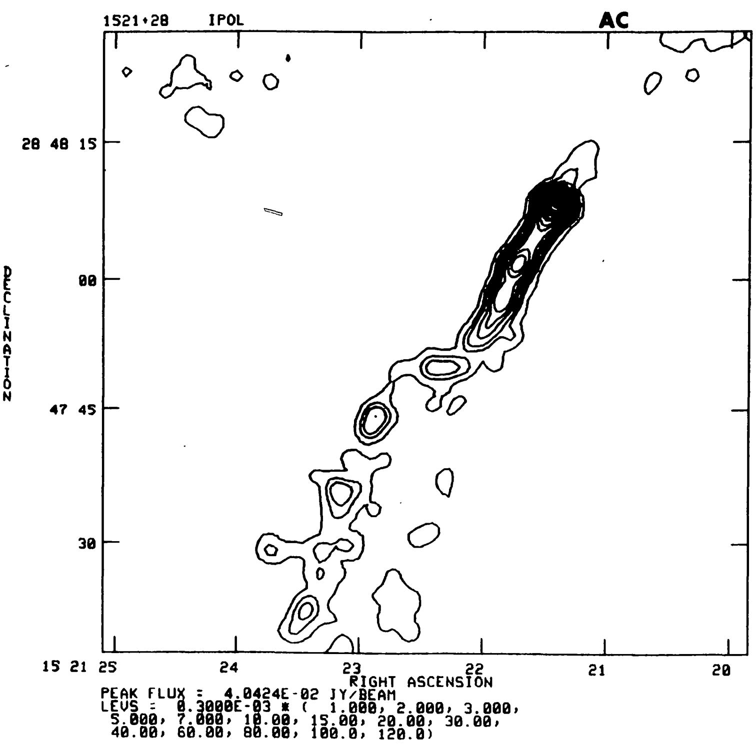

FIGURE 59.

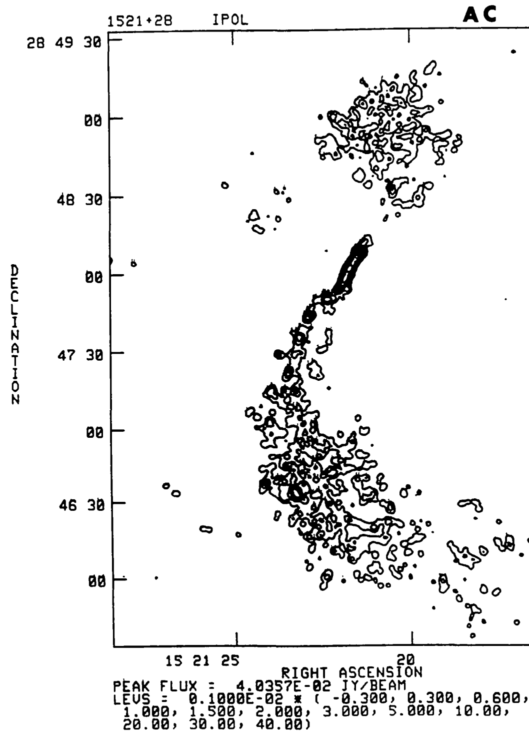

FIGURE 60.

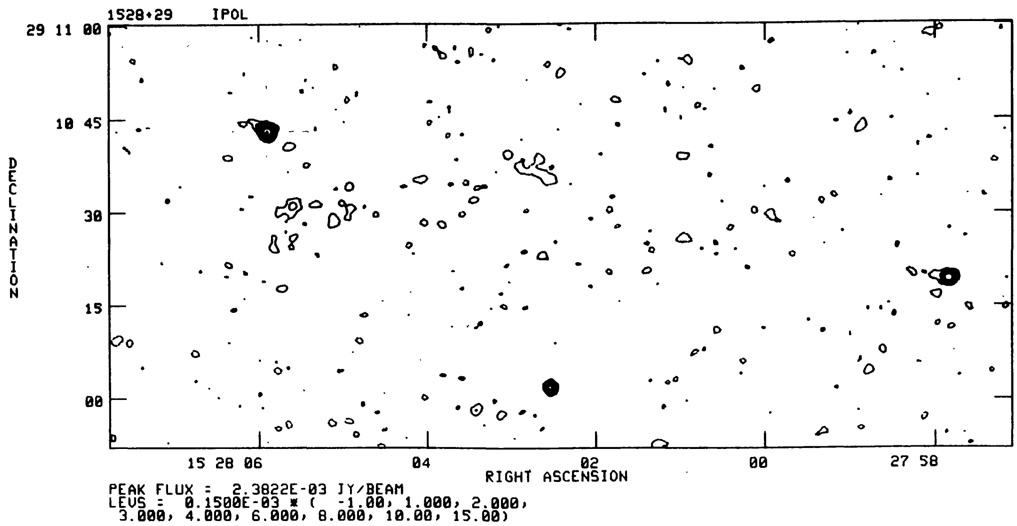

FIGURE 61.

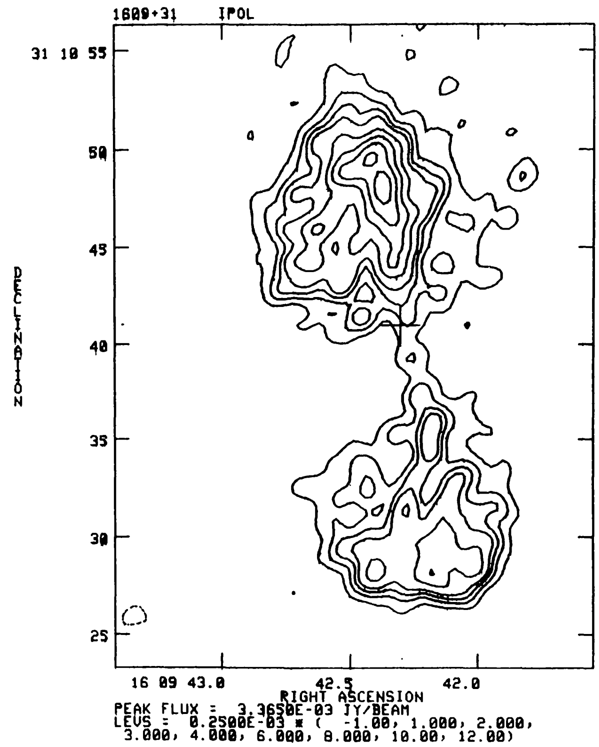

FIGURE 62.

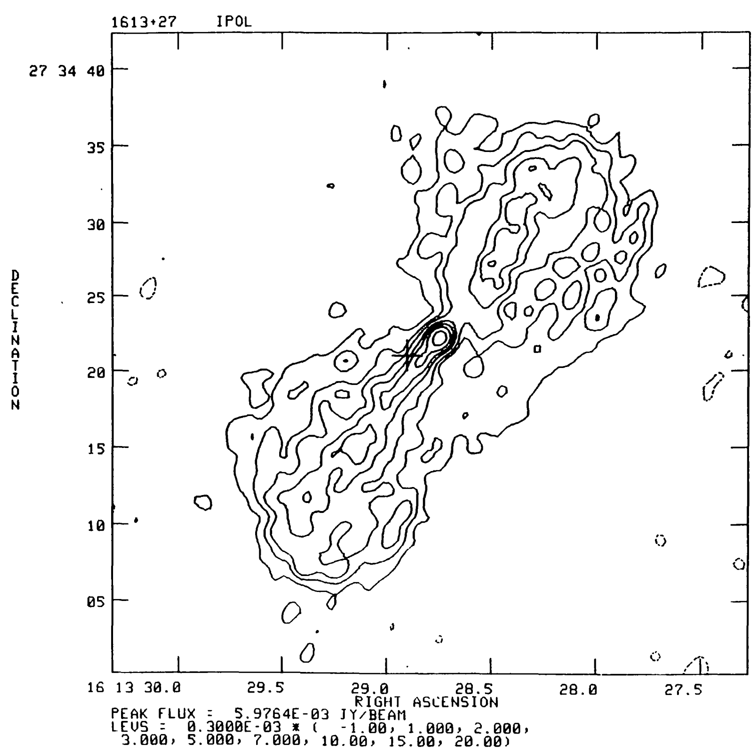

FIGURE 63.

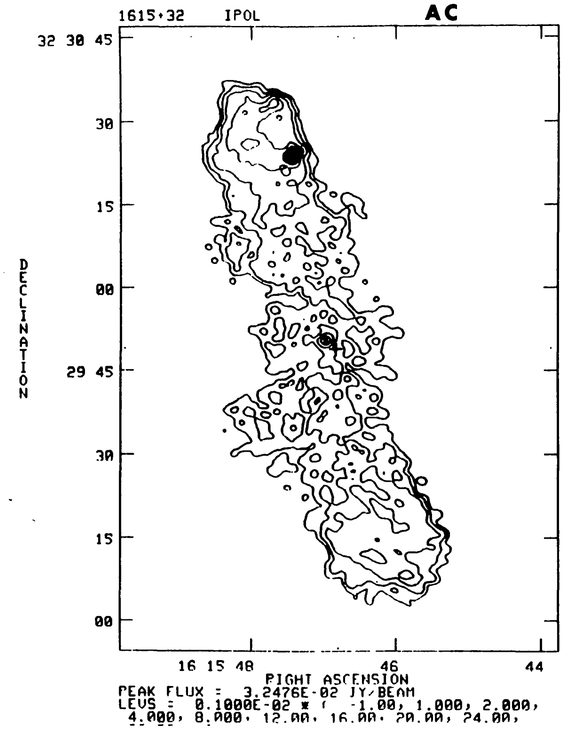

FIGURE 64.

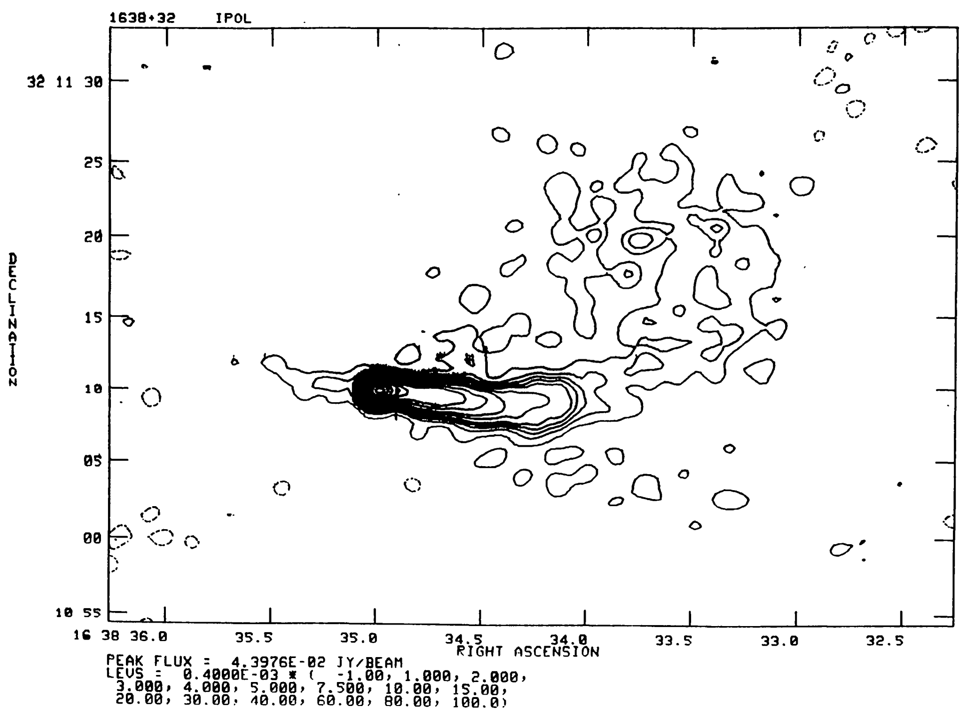

FIGURE 65.

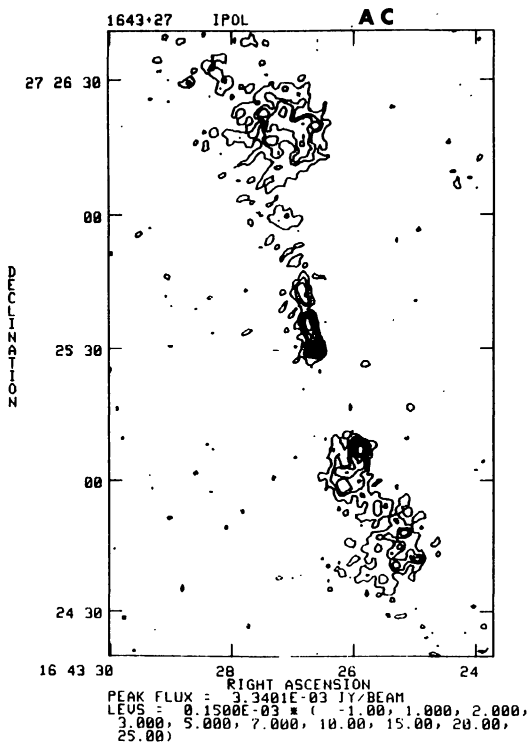

FIGURE 66.

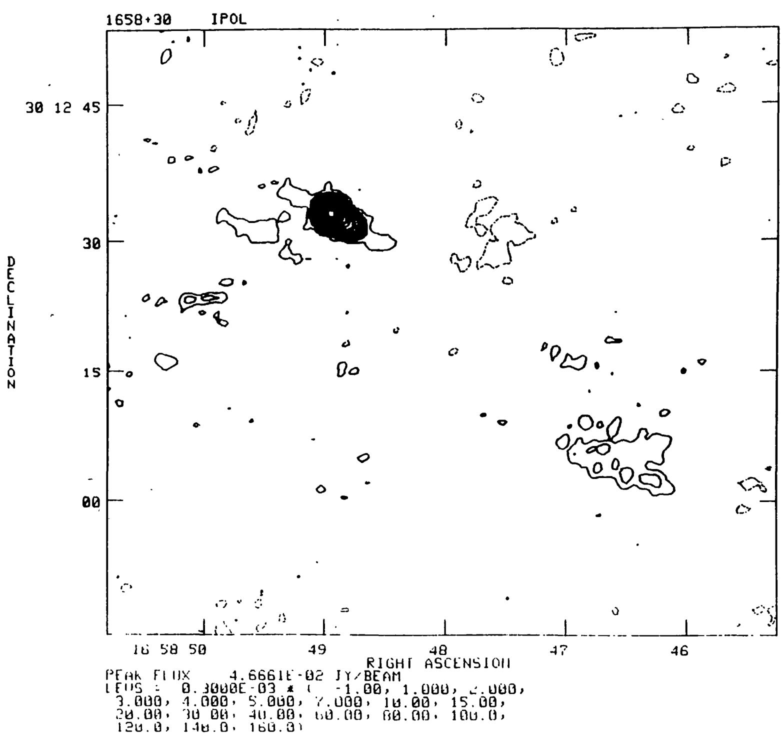

FIGURE 67.

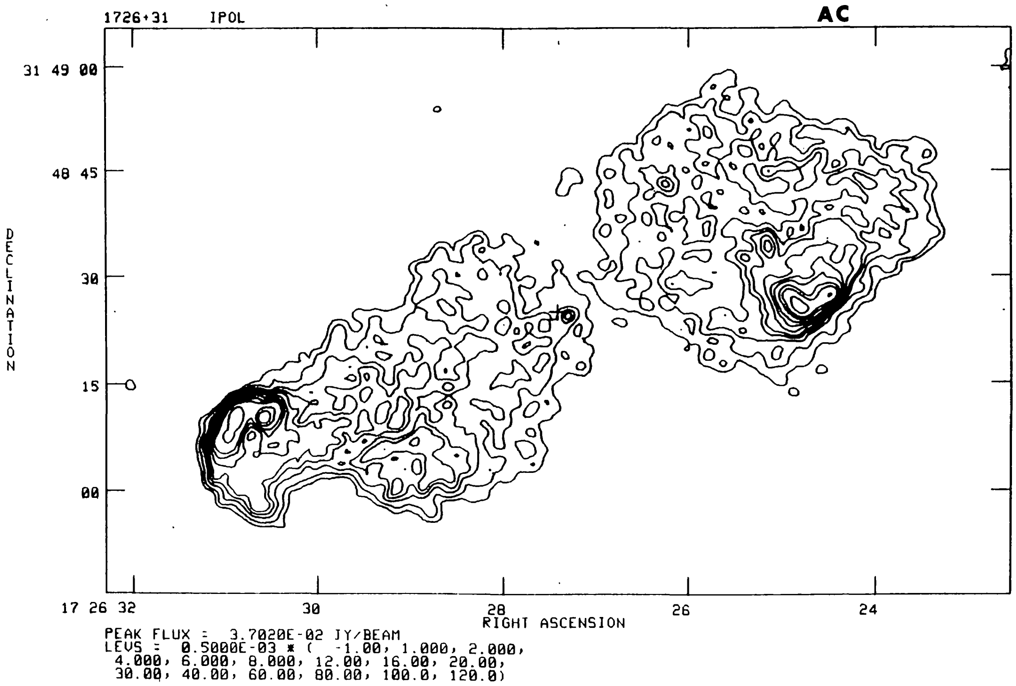

FIGURE 68.

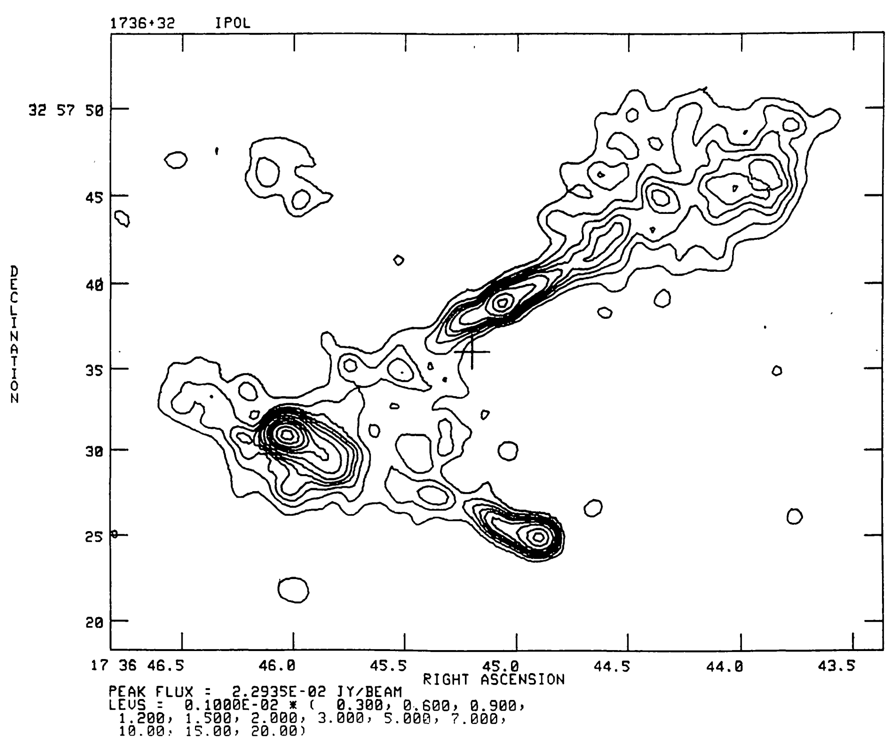

FIGURE 69.

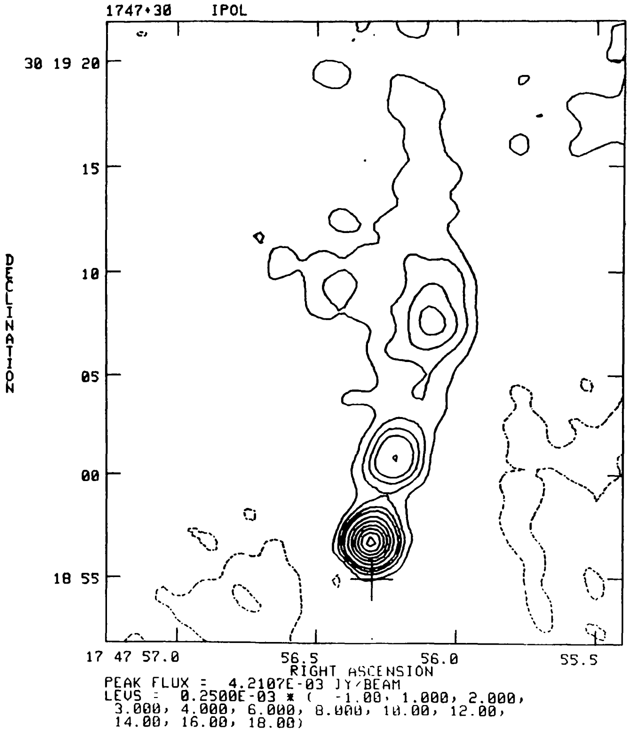

FIGURE 70.

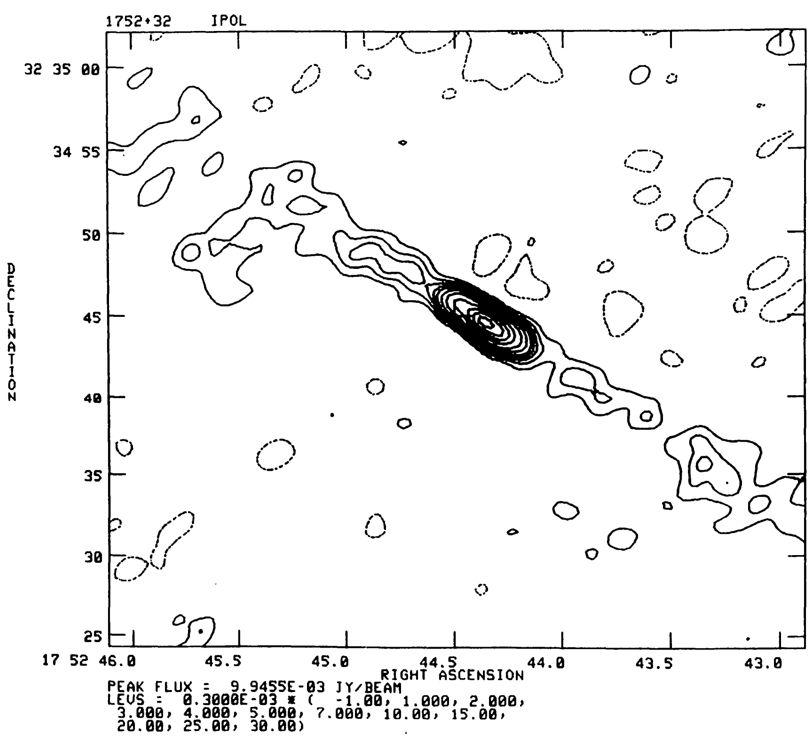

FIGURE 71.

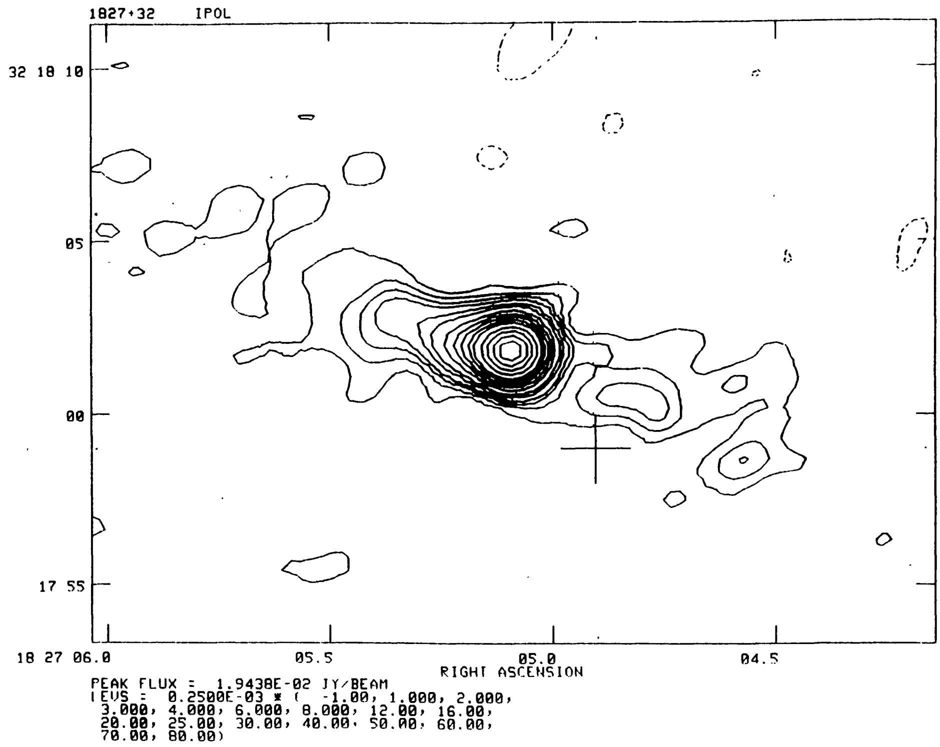
1827+32 IPOL
32 18 10
05
00
17 55
DECLINATION
18 27 06.0
05.5
05.0
04.5
RIGHT ASCENSION
PEAK FLUX = 1.9438E-02 JY/BEAM
LEVS = 0.2500E-03 * (-1.00, 1.000, 2.000,
3.000, 4.000, 6.000, 8.000, 12.00, 16.00,
20.00, 25.00, 30.00, 40.00, 50.00, 60.00,
70.00, 80.00)

FIGURE 72.